Interaction of Nitric Oxide with Cytochrome P450 BM3[†]

Luca G. Quaroni,[‡] Harriet E. Seward,[§] Kirsty J. McLean,[§] Hazel M. Girvan,[§] Tobias W. B. Ost,[||] Michael A. Noble,[⊥] Sharon M. Kelly,[#] Nicholas C. Price,[#] Myles R. Cheesman,[○] W. Ewen Smith,[△] and Andrew W. Munro*,[§]

Elettra Sincrotrone Trieste, 34012 Basovizza, Trieste, Italy, Department of Biochemistry, University of Leicester, The Adrian Building, University Road, Leicester LE1 7HQ, U.K., Department of Chemistry, University of Edinburgh, The King's Buildings, West Mains Road, Edinburgh EH9 3JJ, U.K., Anadys Pharmaceuticals Inc., 6777 Nancy Ridge Drive, San Diego, California 92122, Division of Biochemistry and Molecular Biology, Institute of Biomedical and Life Sciences, University of Glasgow, Glasgow G12 8QQ, U.K., School of Chemical Sciences, University of East Anglia, Norwich NR4 7TJ, U.K., and Department of Pure and Applied Chemistry, The University of Strathclyde, The Thomas Graham Building, Cathedral Street, Glasgow G1 1XL, U.K.

Received April 26, 2004; Revised Manuscript Received October 14, 2004

ABSTRACT: The interaction of nitric oxide with cytochrome P450 BM3 from *Bacillus megaterium* has been analyzed by spectroscopic techniques and enzyme assays. Nitric oxide ligates tightly to the ferric heme iron, inducing large changes in each of the main visible bands of the heme and inhibiting the fatty acid hydroxylase function of the protein. However, the ferrous adduct is unstable under aerobic conditions, and activity recovers rapidly after addition of NADPH to the flavocytochrome due to reduction of the heme via the reductase domain and displacement of the ligand. The visible spectral properties revert to that of the oxidized resting form. Aerobic reduction of the nitrosyl complex of the BM3 holoenzyme or heme domain by sodium dithionite also displaces the ligand. A single electron reduction destabilizes the ferric−nitrosyl complex such that nitric oxide is released directly, as shown by the trapping of released nitric oxide. Aerobically and in the absence of exogenous reductant, nitric oxide dissociates completely from the P450 over periods of several minutes. However, recovery of the nativelike visible spectrum is accompanied by alterations in the catalytic activity of the enzyme and changes in the resonance Raman spectrum. Specifically, resonance Raman spectroscopy identifies the presence of internally located nitrated tyrosine residue(s) following treatment with nitric oxide. Analysis of a Y51F mutant indicates that this is the major nitration target under these conditions. While wild-type P450 BM3 does not form an aerobically stable ferrous−nitrosyl complex, a site-directed mutant of P450 BM3 (F393H) does form an isolatable ferrous−nitrosyl complex, providing strong evidence for the role of this residue in controlling the electronic properties of the heme iron. We report here the spectroscopic characterization of the ferric− and ferrous−nitrosyl complexes of P450 BM3 and describe the use of resonance Raman spectroscopy to identify nitrated tyrosine residue(s) in the enzyme. Nitration of tyrosine in P450 BM3 may exemplify a typical mechanism by which the ubiquitous messenger molecule nitric oxide exerts a regulatory function over the cytochromes P450.

The cytochromes P450 (P450s)[1] are a superfamily of *b*-type hemoproteins catalyzing a vast array of oxidative reactions. The P450s bind and cleave molecular oxygen, usually inserting a single atom of molecular oxygen into the substrate, with the other atom converted into water. Their substrate range is enormous, ranging from simple molecules such as acetone to complex polycyclic species (*1*). They are of huge importance in physiology and medicine, with genetic mutations in P450 (*CYP*) genes known to underlie defects in steroid metabolism and drug metabolism (*2*) and with cytochrome P450-dependent activation of procarcinogens considered to be an important factor in susceptibility to certain cancers (*3*).

Eukaryotic P450s are usually membrane-bound enzymes and interact with membranous redox partners. Bacterial forms (and their redox partners) are generally soluble. The soluble bacterial forms have proved to be the most experimentally

[†] The authors thank the Biotechnology and Biological Sciences Research Council (U.K.) and the Engineering and Physical Sciences Research Council (U.K.) for their support for these studies. A.W.M. thanks the Royal Society for the award of a Leverhulme Trust Senior Research Fellowship. L.G.Q. was funded by a University of Strathclyde Ph.D. studentship award. L.G.Q. thanks NATO for the award of a travel grant to enable studies in Iowa.

* To whom correspondence should be addressed. Tel: +44 116 252 3464. Fax: +44 116 252 3369. E-mail: awm9@le.ac.uk.

[‡] Elettra Sincrotrone Trieste.

[§] University of Leicester.

[||] University of Edinburgh.

[⊥] Anadys Pharmaceuticals Inc.

[#] University of Glasgow.

[○] University of East Anglia.

[△] The University of Strathclyde.

[1] Abbreviations: GSNO, *S*-nitrosylglutathione; MCD, magnetic circular dichroism; NOR1, (D,L)-(*E*)-methyl-2[(*E*)-hydroxyimino]-5-nitro-6-methoxy-3-hexenamide; NOS, nitric oxide synthase; P450, cytochrome P450 monooxygenase; PMSF, phenylmethylsulfonyl fluoride; RR, resonance Raman; SERR, surface-enhanced resonance Raman; SNAP, *S*-nitro-*N*-acetylpenicillamine.

10.1021/bi049163g CCC: $27.50
Published on Web 11/30/2004

tractable systems, and X-ray crystal structures have been obtained from six bacterial P450s (*1*, *4*−8) as well as from inhibitor and substrate-bound forms (e.g., refs *9* and *10*). In addition, the structures of the first eukaryotic cytochromes P450 have been reported recently (*11*). The structure of the human CYP 2C5 enzyme was solved after extensive molecular biology studies to optimize expression of a soluble domain of the enzyme (*12*). As with CYP 2C5, the structure of the CYP 2C9 showed extensive similarity to the bacterial structures already determined, validating the use of the soluble bacterial enzymes for structural and spectroscopic studies to define mechanistic aspects of cytochromes P450 from eukaryotes (*13*, *14*). The most intensively studied P450s are the camphor hydroxylase P450 cam from *Pseudomonas putida* and the fatty acid hydroxylase P450 BM3 from *Bacillus megaterium*. In recent years, the P450 BM3 system has been the subject of intense scrutiny, as it employs a similar electron transfer system to that used by mammalian drug-metabolizing forms (P450 and diflavin P450 reductase). In addition, the fusion of the heme domain of P450 BM3 to its diflavin reductase in a single polypeptide is an arrangement similar to that of the nitric oxide synthases (*15*).

Over the past decade, the importance of the nitric oxide (NO) radical as a regulatory molecule in biological systems has been increasingly recognized (*16*). The multiple functions of NO include roles in vascular relaxation, neuronal signal transmission, and function of the immune system (e.g., ref *17*), and its involvement in pathological states is also currently the subject of intensive research (e.g., ref *18*). NO has long been recognized to bind to hemoproteins (often inhibiting their function) and has been extensively used to probe the active sites of metalloproteins by techniques such as UV−visible spectroscopy (for colored complexes), EPR (as a spin probe in the formation of paramagnetic NO complexes) (*19*), and resonance Raman spectroscopy (*20*). Only relatively recently has it been confirmed that intracellular production of NO and the interactions of NO with proteins have real biological significance. For instance, NO binding to mammalian cytosolic guanylate cyclase leads to activation of the production of the second messenger cGMP (*21*), and the production of NO by macrophages is central to the bactericidal role of these cells (*22*). NO is known to cause autoinhibition of the various eukaryotic forms of the enzyme that catalyze its synthesis (nitric oxide synthase) by simple ligation to the ferrous heme iron (*23*), although the importance of this phenomenon is controversial (*24*). However, the inhibitory action of NO has been demonstrated for many cytochrome P450 monooxygenases (e.g., ref *25*).

The possibility for a role of NO in the regulation of P450s has been postulated [e.g., the negative regulation of steroidogenesis (*26*)], although the mechanisms by which such actions are mediated may not be as simple as the formation of a heme−NO adduct. The inhibition of cytochromes P450 1A1 and 2B1 by NO has been demonstrated to be biphasic, as has the inhibition of the non-P450 hemoproteins lipoxygenase and cyclooxygenase. Only one of these phases (the reversible one) is due to simple heme ligation (*27*, *28*). It was postulated that the second (irreversible) phase was due to modification of amino acid residue(s) of these P450s by nitrogen oxide(s) (e.g., ref *29*). Previously, we have demonstrated the time-dependent formation of nitrotyrosine in CYP2B4 (P450 LM2) after NO treatment and raised the possibility that similar modifications may have general regulatory effects on the P450s (*30*). Already, peroxynitrite has been shown to mediate nitration of tyrosine residues in P450 BM3 and other P450s and to inhibit activity in certain forms (e.g., refs *31* and *32*). However, recent studies suggest that peroxynitrite (which is formed rapidly by reaction between nitric oxide and superoxide and is considered to mediate tyrosine nitration in inflammatory and infectious diseases) may not be a physiologically relevant nitrating agent. Instead, nitrite-dependent peroxidase activity may give rise to protein tyrosine nitration (*33*, *34*).

In this paper we investigate the interaction of nitric oxide with the model cytochrome P450 BM3 system, the spectroscopic features of the NO adducts of the enzyme, and the effects of the interaction on catalysis. We present the first reported CD and MCD spectra for ferrous−nitrosyl [Fe(II)-NO] and ferric−nitrosyl [Fe(III)NO] P450 species, respectively, and show that nitration of P450 BM3 tyrosine residues is a consequence of the aerobic reaction with nitric oxide, using resonance Raman (RR) spectroscopy and the sensitive surface-enhanced RR (SERR) spectroscopy technique to demonstrate tyrosine nitration. We present these RR-based methods as novel and sensitive methods for detection of biologically relevant tyrosine nitration reactions.

EXPERIMENTAL PROCEDURES

Molecular Biology. Escherichia coli strain TG1 [*sup*E, *hsd*Δ5, *thi*, Δ(*lac-pro*AB), F′ (*tra*D36, *pro*AB$^+$, *lac*I^q, *lac*ZΔM15)] was used for all cloning work and for overexpression of intact P450 BM3 and its component heme domains. The preparation of constructs for the overexpression of intact P450 BM3 (constructs pBM25 and pBM23) and of its component heme (P450, residues 1−472; construct pBM20) domains has been presented in previous publications (*35*, *36*). For transformants of pBM20 and pBM25, expression was from inducible (*lac*) promoters. For transformants of pBM23, expression is from the native *Bacillus* promoter in the pUC118 clone and occurs to high levels without induction if growth is continued for 6−8 h after the culture enters stationary phase. Mutants Y51F (in both the intact flavocytochrome P450 BM3 and its heme domain) were generated by oligonucleotide-directed mutagenesis of pBM25 and pBM20 templates, as described previously (*37*−39). Mutants F393H in both flavocytochrome and the heme domain were created in similar fashion, as described previously (*40*).

Enzyme Preparations. Wild-type flavocytochrome P450 BM3 and its component heme domain were expressed and purified essentially as outlined previously (*35*). Induction of expression from pBM25 and pBM20 clones (and the respective Y51F and F393H mutants) was by IPTG addition (500 μg/mL) to cultures grown at 37 °C in Terrific broth, with induction performed at an OD_{600} of 1.0. Thereafter, the temperature was decreased to 30 °C, and culture was continued for a further period of 12 h. Cells were harvested and broken by sonication, and P450 proteins were purified by successive column chromatography steps on DEAE-Sephacel and hydroxyapatite (*35*). A final gel filtration purification step (Sephacryl S-300HR) was used to remove minor contaminating protein species. PMSF (1 mM) and EDTA (1 mM) were added to all buffers to minimize

proteolysis. The Y51F and F393H mutants of the flavocytochrome and heme domain were prepared in identical fashion to the wild-type enzymes. All purified proteins were concentrated by ultrafiltration to a final volume of ~1 mL and then stored at −20 °C after dialysis into a 500-fold volume of buffer A containing 50% glycerol and protease inhibitors. The purified protein was used for experiments within 1 month of preparation.

Spectrophotometric and Kinetic Analysis. All aerobic UV−visible spectra and kinetic data were collected on either a Shimadzu 2401 or a Cary UV-50 Bio (Varian) spectrophotometer using 1 cm path length quartz cells. Enzyme assays to determine the effects of nitric oxide on P450 BM3 catalysis (cytochrome *c* reduction and fatty acid-dependent NADPH oxidation) were performed as described previously (*35*, *39*). Activity was measured at 30 °C in 20 mM MOPS plus 100 mM KCl (pH 7.4) (assay buffer). Substrate-induced changes in absorption spectra (arising from changes in the heme iron spin-state) were used to titrate the interaction of fatty acids with wild-type and Y51F mutants (using ~2−5 μM enzyme), as described previously (*39*). Nitric oxide complexes of the P450s were generated aerobically by brief bubbling of the enzyme solutions (ca. 2−10 μM) with nitric oxide gas (three to five small bubbles only delivered) or by mixing with a 5-fold molar excess of nitric oxide-releasing chemicals (usually PROLI NONOate or *S*-nitrosylglutathione). Spectra were also collected under anaerobic conditions within a Belle Technology glovebox under a nitrogen atmosphere, with oxygen maintained at less than 5 ppm. Degassed, concentrated enzyme samples were passed through an anaerobic Sephadex G25 column (1 × 20 cm) (Sigma) immediately after admission to the glovebox, thereby removing all traces of oxygen. The column was equilibrated and enzyme eluted with deoxygenated assay buffer. Nitric oxide-saturated buffer solutions [1.9 mM (*41*)] were generated by first preparing oxygen-free buffer (100 mM potassium phosphate, pH 7.0) by degassing and bubbling vigorously with oxygen-free nitrogen for 30 min. The buffer was then bubbled with nitric oxide for 30 min. The absence of color in the solution after this time indicated that it was essentially free of nitrite/nitrate. P450−nitrosyl complexes were then generated anaerobically by mixing the P450 and nitric oxide-saturated solutions. Spectra were recorded on a Shimadzu 1201 UV−visible spectrophotometer (typically between 250 and 800 nm) contained within the anaerobic environment. Spectral titration of the Fe(III)NO forms of flavocytochrome P450 BM3 and its heme domain with fatty acid substrate (arachidonic acid) was performed anaerobically using 33 and 6.6 mM ethanolic stocks of arachidonate. Degassed and deoxygenated ethanol was used for dissolving the fatty acid, and total additions were limited to less than 0.25% of the volume of the P450 sample. At these concentrations, ethanol does not affect the catalytic properties of the P450 (*39*). All data manipulations and nonlinear least squares curve fitting of data were conducted using Origin software (Microcal). For the tight-binding fatty acid, data were fitted to eq 1 . The quadratic function accounts for the

$$A_{obs} = (A_{max}/2E_t)(S + E_t + K_d) - ((S + E_t + K_d)^2 - 4SE_t)^{0.5} \quad (1)$$

quantity of enzyme consumed in the enzyme−substrate complex at each point in the titration. In eq 1, A_{obs} is the observed absorption change at substrate concentration S, E_t is the total enzyme concentration, and K_d is the dissociation constant for the enzyme−substrate complex.

The reduced nitrosyl complexes [Fe(II)NO] of P450 BM3 and its F393H mutant were generated either by anaerobic mixing of nitric oxide with the dithionite-reduced P450 or by reduction of the Fe(III)NO complex (either aerobically or anaerobically). Spectral studies to evaluate the formation and stability of these species were performed both aerobically and anaerobically by accumulating several spectra rapidly following initiation of Fe(II)NO complex formation using a Cary UV-50 Bio spectrophotometer (Varian) and anaerobically using an Applied Photophysics SX18MV UV−visible stopped-flow instrument coupled to a photodiode array UV−visible detector. The integrity of cysteinate ligation in the nitrosyl complexes was investigated by taking samples of the Fe(II)NO complexes (both immediately after formation and following extensive reoxidation in air) and mixing with further dithionite reductant in the presence of carbon monoxide. The UV−visible absorption spectrum was then recorded to determine the relative populations of the native P450 and inactive P420 species, which have absorption maxima close to the named wavelengths.

In an experiment to establish whether nitric oxide was released by NADPH-dependent reduction of the ferric−nitrosyl complex of flavocytochrome P450 BM3 (100 μM), enzyme was prepared anaerobically as described above and mixed with the minimum amount of nitric oxide-saturated solution required to convert the enzyme completely to its nitrosyl complex (as determined spectrophotometrically). The Fe(III)NO P450 BM3 complex was then passed through a Sephadex G25 gel filtration column (15 cm × 1 cm) and eluted using anaerobic assay buffer to remove excess nitric oxide. Identical samples of the NO-ligated ferric flavocytochrome P450 BM3 (5 μM) were then placed in two matched quartz 1 mL cuvettes and spectra recorded on a Shimadzu UV-1201 spectrophotometer located in the anaerobic glovebox. To one of the samples was added a sample of the ferric P450 BM3 heme domain (5 μM), and the spectrum of this mixture was recorded 1 min later. The difference in absorption was computed by spectral subtraction. Thereafter, an identical sample of NADPH (200 μM) was added to both cuvettes to reduce completely the flavocytochromes P450. Immediately following addition of NADPH, and again after a further 1 min, the spectra were rerecorded and differences in the heme Soret region noted. These were predominantly due to binding of nitric oxide released from the flavocytochrome by the exogenous BM3 heme domain present in that sample.

To establish the extent of reduction (i.e., one or two electrons) required to displace nitric oxide from the P450 heme iron, the nitric oxide-ligated heme domain of the P450 (100 μM) and the neutral blue semiquinone form of *E. coli* flavodoxin (500 μM) were prepared anaerobically. In the case of the flavodoxin, the protein was titrated with the minimum quantity of sodium dithionite reductant required to convert the enzyme to the maximal feasible amount of the single electron reduced form [~94%, as a result of the magnitude of the difference in reduction potential between the semiquinone and hydroquinone forms (*42*)]. This was done by progressive small dithionite additions, followed by spectral

measurements at each titration point until the absorption peak representative of the semiquinone form at 585 nm was maximal (*42*). Thereafter, flavodoxin semiquinone was separated from residual dithionite and other contaminants by gel filtration within the glovebox, as described above. The samples were then removed from the glovebox, individual spectra of the P450 nitrosyl complex and the flavodoxin semiquinone were recorded, and then the enzymes were mixed in stoichiometric amounts (5 μM each). Absorption spectra were then recorded immediately and at intervals over the next 10 min. In an identical experiment, the absorption change at 435 nm (near the maximum for the P450−NO complex) was recorded continuously for 15 min at 20 °C.

Stopped-Flow Kinetic Studies. Stopped-flow studies of nitric oxide binding to ferrous P450 BM3 were performed under anaerobic conditions within a Belle Technology glovebox under a nitrogen atmosphere, with oxygen maintained at less than 2 ppm. Measurements were made using an Applied Photophysics SX18MV UV−visible stopped-flow instrument at 30 °C in 100 mM potassium phosphate, pH 7.0. P450 BM3 (8 μM) was made anaerobic and reduced by addition of a small excess of sodium dithionite in the glovebox. Nitric oxide-saturated buffer (1.9 mM) was generated by bubbling oxygen-free buffer vigorously with nitric oxide for 15 min. Nitric oxide solutions at various concentrations were prepared through dilutions of the NO-saturated buffer using a gastight syringe (Hamilton) into sealed containers containing oxygen-free buffer. Enzyme was rapidly mixed in the stopped-flow instrument with solutions containing NO at a variety of different concentrations (10−100 μM). Absorption transients at 442 nm were collected and the data fitted to an exponential process. Observed rates were calculated using Spectrakinetics software (Applied Photophysics). Entire UV−visible spectra (800−190 nm) were also collected under similar conditions using the photodiode array attachment on the stopped-flow instrument.

Spectroscopic Characterization. (A) Resonance Raman and Surface-Enhanced Resonance Raman Spectroscopy. Raman spectra in the blue region were recorded using an Anaspec-modified Cary 81 spectrometer. Scattered light was collected at 90° and analyzed by a 1 m double monochromator fitted with a 1800 g/mm grating and a cooled photomultiplier. In an alternative setup, a Renishaw Model 2000 Raman microscope with 180° scattering geometry and a CCD camera as a multichannel detector was employed as an analyzer. The 457.9 nm emission from a Model 2020 Spectra Physics Ar ion laser was used as the exciting source. Raman spectra in the violet region were recorded using the 413.1 nm emission line from a Coherent Innova 200 Kr ion laser. Scattered light was collected and analyzed by a Triplemate triple monochromator fitted with a 1200 g/mm grating. The signal was detected by a Princeton Instruments, liquid nitrogen-cooled, CCD camera (LN/CCD-1100PB).

SERR experiments were performed using a citrate-reduced Lee−Meisel silver colloid (*43*). The protein was added to the buffered colloid and allowed to adsorb by overnight incubation at 4 °C. The sample was later transferred to a quartz cell prior to usage. When required, the cell was fitted with a suba-seal cap, and the sample of adsorbed protein was flushed with a stream of nitrogen. Transfer of nitric oxide (six to eight small bubbles) to the sealed cell was performed using a gastight syringe (Hamilton, Reno, NV). Nitric oxide gas was acquired from Sigma and used as supplied.

(B) Circular Dichroism. Circular dichroism (CD) spectra were recorded at room temperature on either a Jasco J-600 or a Jasco J-810 spectropolarimeter for the heme domains of wild-type P450 BM3 and its F393H mutant in Fe(III) (resting), Fe(III)NO, and Fe(II)NO forms. Enzyme was prepared in 50 mM Tris·HCl buffer (pH 7.5) which was degassed and extensively deoxygenated by bubbling with oxygen-free nitrogen. Samples were sealed from the air using a rubber suba-seal cap, and nitric oxide was added to the anaerobic heme domain by introducing several bubbles of gas into the enzyme solution via a needle passed through the rubber seal. Reductant was also introduced by injection of a 5 μL volume of sodium dithionite (in 5-fold molar excess over the protein and made up in the same deoxygenated Tris·HCl buffer) into the sealed solution of enzyme. Conversion to the Fe(III)NO and Fe(II)NO adducts was confirmed by optical spectroscopy. CD spectra were run immediately after sample preparation in the far-UV (190−260 nm) and near-UV−visible (260−600 nm) regions. Quartz cells of path length 0.02 and 1 cm were used for CD measurements in the far-UV and near-UV−visible regions, respectively.

(C) EPR and MCD Spectroscopy. EPR spectra were recorded using an ER-300D electromagnet and microwave bridge interfaced to an ESP1600 computer (Bruker Spectrospin) and fitted with a liquid helium flow cryostat (ESR-9; Oxford Instruments) and dual-mode X-band cavity (Bruker, type ER4116DM). MCD spectra were recorded using circular dichrographs (Jasco Models J-500D and J-730 for the UV−visible and near-infrared regions, respectively). An Oxford Instruments SM-1 superconducting solenoid with a 25 mm ambient temperature bore was used to generate a magnetic field of 6 T for the room temperature MCD measurements. At room temperature, MCD intensities are linearly dependent on magnetic field and are plotted normalized to magnetic field as $\Delta\epsilon/H$ (M^{-1} cm^{-1} T^{-1}). All samples were contained in anaerobic cells.

For EPR and MCD studies, samples of Fe(II)NO P450s (100 μM enzyme in a 200 μL sample) were prepared by anaerobic reduction of enzyme with stoichiometric quantities of sodium dithionite with stirring for 10 min under an atmosphere of nitric oxide gas. Alternatively, the reduced P450 samples were mixed with a 4-fold molar excess of nitric oxide released from PROLI NONOate (Alexis). Both methods gave complete conversion to the Fe(II)NO adduct for the P450 BM3 F393H mutant. For Fe(III)NO complexes, the oxidized enzymes were stirred under a nitric oxide atmosphere for 10 min. All samples were made up in 50 mM HEPES/D_2O [apparent pH (pH*) = 7.5].

Materials. Molecular biology reagents were from Promega or NEB. Nitric oxide-releasing chemicals [*S*-nitrosylglutathione (GSNO), (±)-(*E*)-methyl-2-[(*E*)-hydroxyimino]-5-nitro-6-methoxy-3-hexenamide (NOR-1), sodium nitroprusside (SNP), and *S*-nitrosylacetylpenicillamine [SNAP)] were from Calbiochem. PROLI NONOate was from Alexis Biochemicals. Nitrotyrosine was from Cayman Chemical Co. Unless otherwise stated, other reagents were purchased from Sigma (Poole, Dorset) and were of the highest grade available.

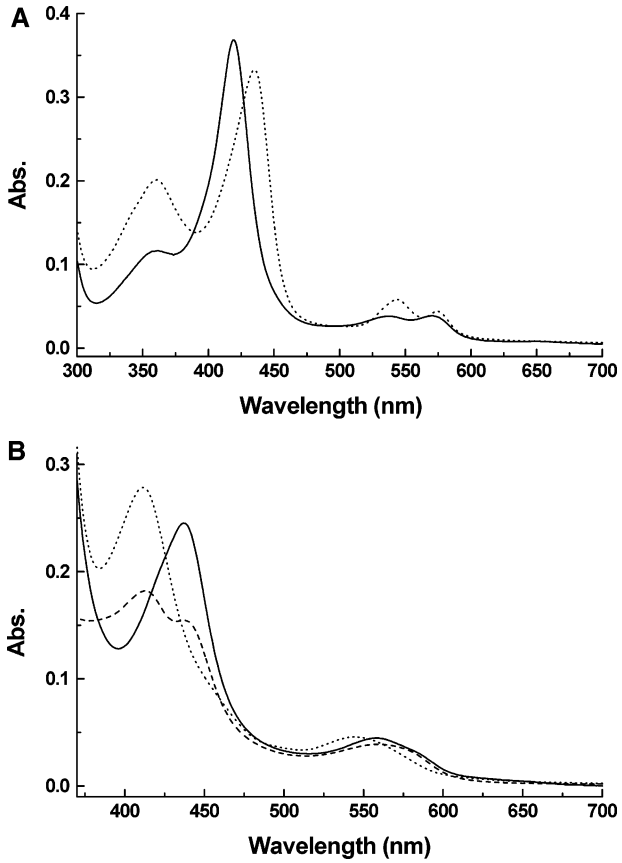

FIGURE 1: UV−visible spectra of the P450 BM3 heme domain and nitrosyl adducts. (A) Visible spectra of the oxidized (solid line) and Fe(III)NO adduct (dotted line) for the wild-type P450 BM3 heme domain (3.9 μM). Spectral features for the F393H mutant heme domain Fe(III)NO complex are essentially the same as those for the wild type, with the Soret band centered at 435 nm. (B) Visible spectra for the Fe(II) (dotted line) and Fe(II)NO (solid line) forms of the F393H mutant heme domain (3.9 μM). The dashed line shows the spectrum recorded for the Fe(II)NO complex of the wild-type heme domain (also 3.9 μM) immediately after anaerobic addition of nitric oxide to ferrous heme. The spectrum indicates that, due to the instability of the Fe(II)NO adduct in wild-type P450 BM3, there is only partial conversion to this species at equilibrium. Data were collected as described in the Experimental Procedures section.

RESULTS

Spectrophotometric Properties of P450−NO Complexes. The binding of nitric oxide to the P450 BM3 heme iron induced large absorbance shifts in the UV−visible absorption spectrum. On binding of NO to the oxidized (ferric) enzyme, the Soret band was shifted from 419 to 435 nm. There was also a large increase in intensity of the α and β bands of the heme and a shift in their absorbance maxima to 575 and 543 nm, respectively (Figure 1A). The shoulder on the short-wavelength side of the Soret band in oxidized P450 BM3 becomes a distinct, broad peak in the Fe(III)NO complex, with an absorption maximum at 360 nm. Essentially identical spectral perturbations were observed for both intact P450 BM3 and for its heme domain. Similar spectra were generated by addition of the nitric oxide donors *S*-nitrosylglutathione (GSNO), (±)-(*E*)-methyl-2-[(*E*)-hydroxyimino]-5-nitro-6-methoxy-3-hexenamide (NOR-1), PROLI NONOate, and sodium nitroprusside (SNP). *S*-Nitrosylacetylpenicillamine (SNAP) did not appear to induce complete conversion to the Fe(III)NO adduct, presumably due to the slow reoxidation of the adduct (see below) that competes with the relatively slow release of NO by SNAP under the conditions used. The spectral features of the Fe(III)NO form of P450 BM3 are shown in Table 1 and are compared with those from other P450s and from isoforms of nitric oxide synthase (NOS), which are eukaryotic flavocytochrome relatives of P450 BM3 with cysteinate-ligated heme iron (*44*). Attempts to determine the affinity of NO for ferric P450 using anaerobic spectral titration of the P450 with small volumes of nitric oxide-saturated buffer were not successful due to the very tight binding of the ligand. However, these experiments did serve to demonstrate that the K_d is significantly lower than the minimum concentration of P450 required to provide an adequate spectral signal; i.e., K_d is ≪500 nM. When the aerobically prepared Fe(III)NO complex of P450 BM3 was left in air to reoxidize, the Soret band was seen to shift back completely to 419 nm over a period of approximately 1 h. This reflects the irreversible reaction of dissociated nitric oxide with oxygen in solution. The pH of the buffered solution did not decrease significantly on addition of these small amounts of NO gas required to cause complete conversion to the ferric−NO form. However, it was noted that excessive addition of NO to the buffer resulted in large decreases in pH, which brought about protein denaturation and precipitation, and the development of an absorption spectrum characteristic of nitrous acid in the 250−350 nm range.

Table 1: Visible Spectroscopic Properties of the Ferric [Fe(III)NO] and Ferrous [Fe(II)NO] Forms of Nitric Oxide-Ligated Cytochromes P450 and Nitric Oxide Synthases

	Fe(III)NO		Fe(II)NO	
enzyme	Soret	visible	Soret	visible
P450 BM3	435	543, 575	437	559
P450 cam[a]	430	541, 571	438	557
P450 1A2[b]	431	541, 571	400	552
P450 LM[a]	436	543, 574	444	585
P450 2B4[c]	433	543, 575		
P450 1A2[c]	433	542, 571		
nNOS[d]	440	549, 580	436	567
iNOS[e]	443	549, 585	436	560

[a] *P. putida* cytochrome P450 cam and for rat liver P450 LM from ref *19*. [b] Rat P450 1A2 from ref *77*. [c] Rabbit P450 2B4 (P450 LM2) and P450 1A2 (P450 LM4) from ref *79*. [d] Rat neuronal nitric oxide synthase (nNOS) from ref *23*. [e] Murine inducible NOS (iNOS) from ref *80*. In the case of the data for the (1) Fe(III)NO and (2) Fe(II) NO complexes for P450 LM, the band positions are those determined from peaks in the difference spectra generated by subtraction of (1) the spectrum of the ferric enzyme from that of the Fe(III)NO complex and (2) the spectrum of the ferrous enzyme from that of the Fe(II)NO complex.

Attempts to isolate the Fe(II)NO form of P450 BM3 under aerobic conditions were largely unsuccessful due to the apparent instability of this species. A spectrum collected immediately following addition of dithionite to an Fe(III)-NO wild-type P450 BM3 heme domain sample showed that the Soret band was located at ∼420 nm, with a significant shoulder at ∼438 nm and sharply split features in the α/β region. With reference to Figure 1A, this indicated that the Fe(II)NO form had rapidly converted into a spectral mixture of the ferric and Fe(III)NO forms. Attempts to reduce the enzyme aerobically prior to addition of nitric oxide were also unsuccessful due to the rapid autoxidation of ferrous P450 BM3 (*45*). Instead, attempts were made to isolate the Fe-

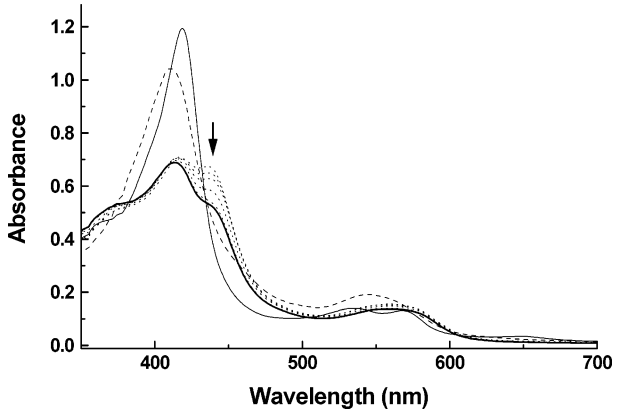

FIGURE 2: Spectral changes following reaction of ferrous P450 BM3 with nitric oxide. The spectrum of the wild-type P450 BM3 heme domain (12 μM) is shown in the ferric (thin solid line) and anaerobically dithionite-reduced ferrous (dashed line) forms. After formation of the ferrous form, the protein was mixed with nitric oxide, and spectra were collected immediately and at 1 min intervals over the following 5 min (dotted lines, with the final spectrum at 5 min shown as a thick, solid line). The arrow shows the direction of absorption change occurring at ~437 nm [near the spectral maximum for the Fe(II)NO form] over the time period. On subsequent anaerobic incubation for a further 10 min, there was negligible change observed from the final spectrum shown here.

(II)NO complex of wild-type P450 BM3 under anaerobic conditions. The ferrous P450 BM3 heme domain was generated in the glovebox by dithionite reduction, and complete conversion to the ferrous form was confirmed by the shift of the Soret band of the P450 to ~410 nm over a period of up to ~5 min (*40*). Thereafter, excess dithionite was removed from the P450 by anaerobic gel filtration using Sephadex G25 resin, and the Fe(II)NO complex formed by mixture with anaerobic NO-saturated buffer, as described in the Experimental Procedures section. While the overall phenomenon observed under anaerobic conditions was similar in terms of the instability of the Fe(II)NO complex, performing the reaction in the glovebox resulted in a different final spectral form. Thus, anaerobic reaction of ferrous P450 BM3 with NO resulted in the spectral properties of the heme changing rapidly to those apparently reflecting a mixture containing some NO-ligated iron, but primarily non-NO-coordinated P450 in ferric and ferrous forms (Figure 1B). The spectral features of this species in the α/β region (between 500 and 600 nm) are more similar to those for the ferrous form of the enzyme than for the ferric (compare data in panels A and B of Figure 1), suggesting that the ferrous form predominates. To further examine the phenomenon, spectra were collected at regular intervals following the initiation of the anaerobic reaction of the ferrous P450 BM3 heme domain with NO. Spectra are shown in Figure 2, demonstrating the final spectral interconversions that occur as the system reaches equilibrium. From the partially converted Fe(II)NO spectrum for the wild-type P450 BM3 (Figure 2 and Figure 1B), spectral maxima for the Fe(II)NO enzyme form were located at 437 nm (Soret) and at 559 nm in the region of the heme α and β bands. Both maxima are at slightly longer wavelength than those reported previously for P450 cam (*19*) (Table 1).

Recently, it was demonstrated that phenylalanine 393 is a key residue in controlling the electronic properties of the P450 heme iron, such that the reduction potential of the heme iron in the site-directed mutant F393H is increased by almost 100 mV (from -427 ± 4 to -332 ± 6 mV) and its reactivity with molecular oxygen is diminished (*40*). Electronic absorption spectra collected for the Fe(III)NO and Fe(II)NO complexes of the F393H heme domain were essentially identical to those for wild-type P450 BM3 (Table 1). However, presumably as a result of the altered electronegativity of the F393H heme, the stability of the ferrous−NO form was greatly increased in this mutant. The Fe(II)NO complex was stable indefinitely under anaerobic conditions and was even stable for several minutes when generated in air (Figure 1B).

On the basis of an extinction coefficient of 95 mM^{-1} cm^{-1} for the Soret maximum in the oxidized P450 BM3 heme domain, the relative coefficients for the Fe(III)NO and Fe(II)NO species are 86 mM^{-1} cm^{-1} at 435 nm and 63 mM^{-1} cm^{-1} at 437 nm, respectively, and are of apparently equal magnitude for both wild-type and F393H P450 BM3 heme domains.

Dissociation of Nitric Oxide from Ferric P450 BM3. It was observed that the nitric oxide complex of ferric P450 BM3 decomposed spontaneously in aerobic solution over periods of several minutes, leading to the restoration of heme spectral properties typical of the oxidized form of the enzyme. Clearly, NO binding to the ferric heme is reversible, and its reassociation is competitive with the reaction of NO with oxygen in solution. Ultimately, the latter reaction pathway exhausts the NO in solution, and the aqua-ligated P450 species is re-formed. However, reducing agents (either dithionite or NADPH for the intact flavocytochrome P450 BM3) caused similar spectral changes immediately after aerobic addition. As indicated above, the instability of the Fe(II)NO complex suggested that nitric oxide might simply be released from the heme on addition of an electron to the Fe(III)NO complex. Addition of NAD(P)H to the Fe(III)-NO heme domain complex did not result in its dissociation, indicating that the P450 BM3 heme domain does not act as a nitric oxide reductase in a fashion similar to P450 nor from *Fusarium oxysporum* (*4*). However, the fact that NADPH was able to dissociate the Fe(III)NO complex of flavocytochrome P450 BM3 was of particular interest, since addition of this cofactor does not result in the reduction of ferric P450 BM3 heme in the absence of fatty acid substrate, probably mainly due to the unfavorably low (negative) heme iron reduction potential with respect to that of the FMN flavin and NADPH (-427 ± 4 mV for heme iron; cf. -320 mV for NADPH and -213 ± 5 mV for the BM3 reductase FMN oxidized/semiquinone couple) (*38*, *43*). Evidently, NADPH-dependent electron transfer to heme in the Fe(III)NO flavocytochrome P450 BM3 complex can occur via the reductase flavins, but direct reduction of the heme domain by NADPH does not occur. This likely indicates that the heme iron reduction potential of the Fe(III)NO complex is considerably more positive than that of the resting aqua-ligated form.

To establish whether NADPH-dependent reduction of the flavocytochrome P450 ferric−NO complex resulted in direct release of nitric oxide, we set up a reaction system in which two cuvettes containing anaerobically prepared Fe(III)NO flavocytochrome P450 BM3 (5 μM) were placed in the sample and reference compartments of a Shimadzu 2101 spectrophotometer. An equivalent quantity of the ligand-free

ferric heme domain of P450 BM3 was added to front cuvette, and the absorbances zeroed against each other. Thereafter, an excess of NADPH (200 μM) was added to both cuvettes. A difference spectrum was then recorded immediately (between 700 and 300 nm) and again after 1 min. The two spectra were essentially identical and displayed a strong peak at ~434 nm in the solution to which the ligand-free heme domain had been added. This indicated that nitric oxide had been released by the reduced flavocytochrome P450 and that this NO had been "captured" by the heme domain in the sample cuvette. The proportion of the BM3 heme domain converted to its ferric−NO adduct was greater than 85%.

To verify that the process of displacement of NO from the P450 heme required only a single electron (NADPH is a two-electron donor), the Fe(III)NO form of the P450 BM3 heme domain was mixed aerobically with the one-electron-reduced (air-stable blue semiquinone) form of *E. coli* flavodoxin (*42*), as described in the Experimental Procedures section. The flavodoxin semiquinone induced displacement of NO from the P450 domain, with reoxidation of both heme and flavodoxin observed from spectrophotometric measurements made over the next 10 min until the reaction approached completion. The result confirmed that only a single electron was required. However, the rate of the slow reaction was constant, as monitored by the decrease in absorbance at 434 nm. This apparent zero-order process is consistent with a structural change in the protein accompanying NO displacement.

Stopped-Flow Analysis of NO Binding to Ferrous P450 BM3. In view of the apparent instability of the Fe(II)NO complex of P450 BM3, we undertook stopped-flow mixing studies to determine the rate of binding of NO to the ferrous P450 heme iron across a range of NO concentrations (10−100 μM). Preliminary stopped-flow diode array spectrophotometric analysis indicated that 442 nm was an appropriate wavelength to follow the transient formation of the Fe(II)-NO complex. Typically, reactions were analyzed over period of 10−1000 ms, as described in the Experimental Procedures section. With the F393H mutant of the P450 BM3 heme domain, the formation of the Fe(II)NO species was clearly observed due to the relative stability of the complex. Individual ΔA_{442} data were fitted to an exponential function, as described previously (*46*). A plot of the observed rates (k_{obs} values) versus the applied NO concentration was linear [as found also for, e.g., iNOS (*46*)], and an apparent bimolecular rate constant of $(8.54 \pm 0.45) \times 10^6$ M^{-1} s^{-1} for binding of NO (k_{on}) was determined from the gradient of the line. The plot had a positive intercept on the *y*-axis, from which an apparent NO dissociation rate (k_{off}) of 87.8 ± 26.6 s^{-1} was determined. The apparent K_d for the interaction of NO with the ferrous F393H P450 was determined from the ratio of these two values (k_{off}/k_{on}) to be 10.3 μM. A similar set of experiments was performed for the wild-type P450 BM3 heme domain. However, in this case it was found that the formation of the Fe(II)NO complex was transient and that the absorption increase was essentially complete within 50 ms. This phase was immediately followed by an exponential decay of the absorption, which was complete within 1 s of initiating the reaction. The latter phase reflects the collapse of the Fe(II)NO complex (described above). As with the data sets for the F393H enzyme, a plot of k_{obs} versus applied NO concentration (obtained by fitting the A_{442} increase phase) was linear within the range analyzed. Parameters of $k_{on} = (4.67 \pm 0.15) \times 10^6$ M^{-1} s^{-1} and $k_{off} = 13.8 \pm 6.9$ s^{-1} were extracted from the graph. The K_d (k_{off}/k_{on}) was determined to be 3.0 μM. Analysis of the rate of the absorption decrease occurring over the longer time scale (up to 1 s) as the Fe(II)NO species collapses revealed that it showed no apparent dependence on NO concentration, occurring at 10 ± 2 s^{-1}.

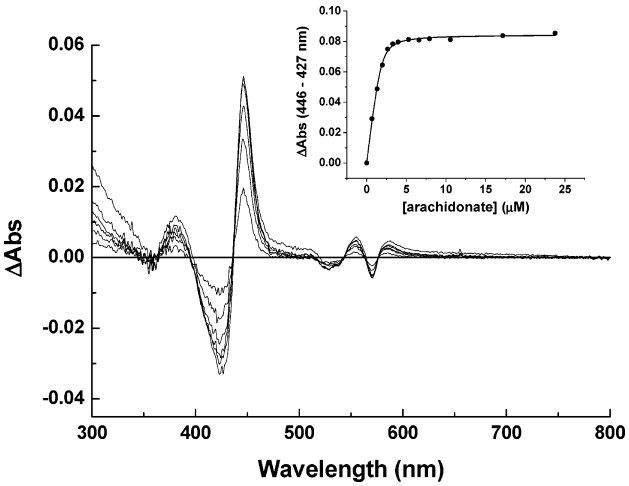

FIGURE 3: Spectral perturbation of the Fe(III)NO adduct of the wild-type P450 BM3 heme domain by fatty acid substrate. Addition of fatty acids induces small shifts in the visible spectrum of Fe(III)NO P450 BM3, with the Soret band shifting from 435 to 437 nm. The main figure shows selected absorption difference spectra for the Fe(III)NO heme domain complex (5 μM) after addition of quantities of arachidonic acid between 0.7 and 26 μM. The inset shows a plot of the induced absorption difference versus arachidonic acid concentration, with the data fitted to eq 1 to yield a K_d value of 0.15 ± 0.03 μM.

Substrate-Dependent Perturbation of the NO-Bound Spectrum by Fatty Acid. In experiments where fatty acid substrates (arachidonic acid and lauric acid) were added to the Fe(III)NO complex of P450 BM3, it was observed that addition of substrate caused a small perturbation of the spectral properties of the complex, with an ~2 nm shift of the Soret absorption maximum from 435 to 437 nm and similar small shifts of the α and β bands (to 576 and 545 nm, respectively). To demonstrate that this spectral perturbation related directly to the binding of substrate in the active site of the P450, we performed substrate-binding titrations of the heme domain Fe(III)NO complex with arachidonic acid under anaerobic conditions [to prevent any reoxidation of the Fe(III)NO complex over the ~30 min period required to complete the titration] (Figure 3). Difference spectra at each point in the titration were generated by subtraction of the starting absolute spectrum from spectra recorded at the relevant point. The apparent dissociation constant for the binding of arachidonate was then determined by plotting the maximal Soret region absorption change from each difference spectrum ($A_{446} - A_{427}$) against the relevant concentration of arachidonate. The plot described a hyperbola, and data were fitted to eq 1. This yielded a K_d of 0.15 ± 0.03 μM. This value is rather tighter than previous estimates for the binding of arachidonate to oxidized, aqua-ligated P450 BM3 (~2−5 μM) (*45*, *47*). This can be explained at least partially by the use of the more accurate eq l (rather than fitting to a simple hyperbolic function) to fit the data. However, another possible explanation for the tighter apparent binding of

arachidonate could relate to the conformational state of the P450. In recent studies of a A264E mutant of P450 BM3, we have shown that long-chain fatty acids bind more tightly than is the case for wild-type P450 BM3 (*48*). In addition, structural studies show that the substrate-free A264E heme domain adopts the conformation previously considered to be a consequence of substrate docking (*49*). Potentially, the conformational state of the enzyme is altered in a similar fashion in the nitrosyl complex of wild-type P450 BM3, and this leads to the apparent enhancement of binding of arachidonate. In recent studies of the resonance Raman properties of the nitrosyl complexes of P450 BM3, Deng et al. described an apparent lack of perturbation of the resonance Raman spectrum of the P450 BM3 heme domain after the addition of fatty acid (palmitate) to the Fe(III)NO heme domain complex (*50*). However, our work demonstrates that small perturbations in the electronic spectrum are observed when substrate binds to the Fe(III)NO heme domain. It is plausible that these reflect environmental changes around the nitrosyl ligand on binding fatty acid.

CD Spectroscopy. Circular dichroism (CD) spectra were recorded for the wild-type and F393H P450 BM3 heme domains in both far-UV (190−260 nm, ca. 3 μM P450) and near-UV−visible (260−600 nm, ca. 20 μM P450) regions. The Fe(III)NO and Fe(II)NO far-UV CD spectra of the P450s were not significantly different from those of the ferric oxidized P450s. Similarly, addition of arachidonate (20 μM) to the Fe(III)NO complexes of wild-type and F393H heme domains did not induce significant changes in the far-UV CD spectra, indicating that the changes observed in the electronic absorption spectra do not reflect any perturbations to secondary structure. Considerable spectral changes are observed in the near-UV−visible CD spectra of the heme domains on ligation with nitric oxide. Previously, we have published the near-UV−visible CD spectra for wild-type oxidized P450 BM3, which shows a prominent broad spectral feature with negative ellipticity in the region of the Soret band of the P450 (*36*). This band is centered at 410 nm for the oxidized wild-type BM3 heme domain and at 413 nm for the F393H heme domain. CD spectral changes induced by addition of nitric oxide were essentially identical for both enzymes, with the band decreasing in intensity and shifting to ca. 432 nm. Due to its inherent instability, it did not prove feasible to obtain a visible CD spectrum for the completely converted Fe(II)NO complex of wild-type P450 BM3. However, satisfactory spectra for the Fe(II)NO form of the F393H heme domain could be collected, with the complete conversion to the Fe(II)NO form confirmed by electronic absorption spectroscopy (Figure 4). The Soret CD bands of these nitrosyl complexes decreased in intensity compared with the unligated P450 heme domain and were shifted to 436 nm. Smaller features of negative ellipticity are seen in the region of the P450 heme α and β bands, with minima located at ca. 582 nm [Fe(III)], 572 nm [Fe(III)NO], and 589 nm [Fe(II)NO]. To our knowledge, this is the first reported near-UV−visible CD spectrum for an Fe(II)NO P450 complex.

Resonance Raman and Surface-Enhanced Resonance Raman Spectroscopies Provide Evidence for P450 Tyrosine Nitration. Resonance Raman (RR) and surface-enhanced RR (SERR) spectra were successfully obtained for both the oxidized heme domain of P450 BM3 and for the Fe(III)NO

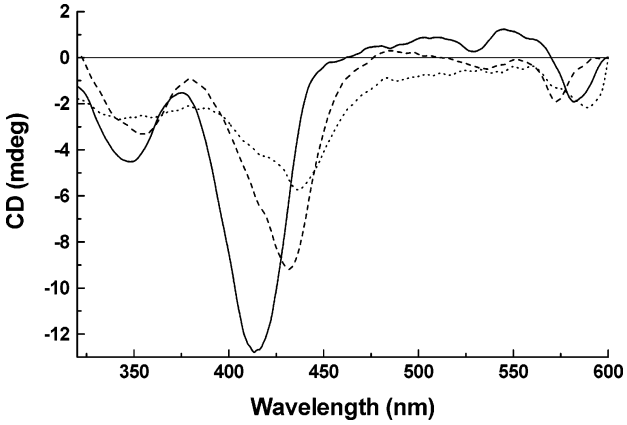

FIGURE 4: Near-UV−visible CD spectra for the F393H mutant of the P450 BM3 heme domain. Spectra were recorded for the oxidized (solid line), Fe(III)NO (dashed line), and Fe(II)NO (dotted line) enzyme forms. The enzyme concentration was 20 μM, and spectra were collected at ambient temperature as described in the Experimental Procedures section. Qualitatively similar data were collected for oxidized [Fe(III)] and Fe(III)NO forms of the wild-type P450 BM3 heme domain. Instability of the Fe(II)NO complex of wild-type P450 BM3 prevented collection of CD data for this species.

form. RR on the oxidized form was performed with laser excitation at 413 nm on 1 mM solutions of the heme domain in 50 mM MOPS (pH 7.4). The NO-treated enzyme was analyzed with excitation from laser lines at both 413 and 457.9 nm. SERR spectra of the oxidized and NO-bound heme domain were obtained as described previously with laser excitation at 457.9 nm (*51*). In agreement with earlier reports, the RR spectrum of the oxidized heme domain was predominantly low spin, while the SERR spectrum of the surface-adsorbed domain had a roughly equal proportion of low-spin and high-spin heme iron (*35*, *51*). The larger proportion of high-spin heme iron in the SERR spectrum results from surface adsorption of the protein. We have shown previously that there is negligible P420 present following surface adsorption (*51*). The presence of the oxidation state marker band ν_4 at 1372 cm^{-1} in both RR and SERR spectra indicates that the ferric oxidation state is retained upon adsorption, and it has been demonstrated previously that substrate- and inhibitor-dependent signals typical of the solution state enzyme occur with the surface-adsorbed P450 (*51*, *52*).

SERR spectra of the BM3 heme domain (1 μM) in both the oxidized form and after the aerobic addition of NO gas and incubation for 1 h at ambient temperature were obtained using excitation at 457.9 nm (Figure 5A,B). The SERR difference spectrum after aerobic NO treatment was generated by subtraction of the spectrum for the oxidized P450 from that of the Fe(III)NO form. The difference spectrum (Figure 5C) shows prominent bands at 1328, 1576, and 1631 cm^{-1}. These vibrations can be assigned to the asymmetric stretching of the nitro group of nitrotyrosine (1328 cm^{-1}) and to the breathing vibrations of the aromatic ring of nitrotyrosine (1576 and 1631 cm^{-1}), clearly indicating the formation of this species after the aerobic reaction of NO with P450 BM3. These features are also clearly seen in the spectrum of pure nitrotyrosinate (Figure 5D). The formation of nitrotyrosine was not observed under anaerobic conditions or by addition of peroxynitrite to this system (100 μM) over the same experimental time. The results from this study suggest that the sharp nitrotyrosinate signal from P450 BM3

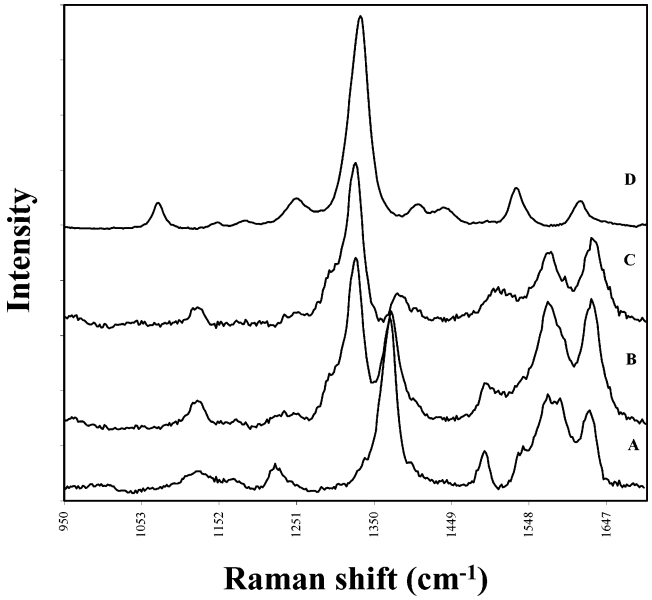

FIGURE 5: Surface-enhanced resonance Raman (SERR) spectra demonstrating nitric oxide-dependent tyrosine nitration of the heme domain of P450 BM3. Spectrum A: SERR of the heme domain of P450 BM3 on a Lee−Meisel colloid, pH 5.8. Spectrum B: SERR of the heme domain of P450 BM3 after aerobic exposure to NO. Spectrum C: The difference spectrum generated by subtraction of spectrum A from spectrum B. Spectrum D: Resonance Raman spectrum of the nitrotyrosinate anion (100 μM). Conditions were as described in the Experimental Procedures section with the P450 BM3 heme domain concentration at 1 μM. Excitation was at 457.9 nm. The large band at 1329 cm^{-1} in the difference spectrum is indicative of tyrosine nitration of P450 BM3.

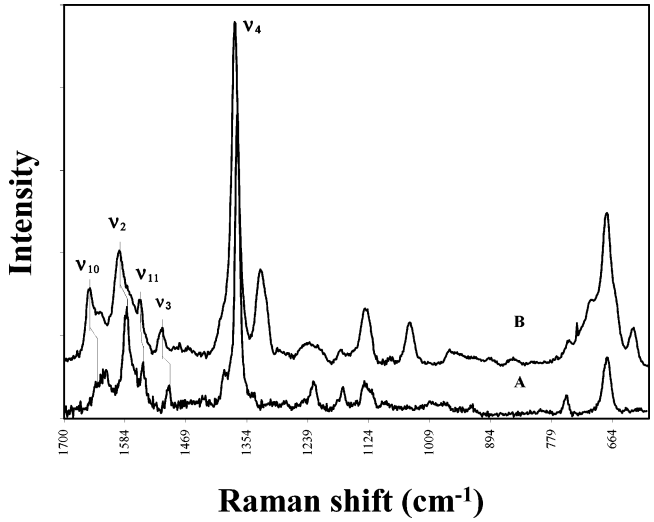

FIGURE 6: Resonance Raman spectrum of the heme domain of P450 BM3 (500 μM) before (A) and after (B) the aerobic addition of NO gas. The sample preparation is detailed in the Experimental Procedures section. The samples were frozen at 77 K for the spectroscopic analysis. Excitation was at 406.7 nm, 40 mW. Nitric oxide-induced band shifts are discussed in the Results section.

arises from only one modified tyrosine. Previous studies of the frequencies of the nitro stretch of nitrophenols in organic solvents (~1325 cm^{-1}) compared with those in water (~1335 cm^{-1}) showed significant shifts depending on the dielectric constant of the solvent (*53*). The relatively low frequency in P450 BM3 suggests that the nitrotyrosine is in a quite hydrophobic location. The nitro stretching frequency increases for the protonated form in hydrogen-donating solvents (*53*). One obvious candidate residue is tyrosine 51 near the mouth of the active site cleft of P450 BM3 (*8*). To assess the possibility that tyrosine 51 was a target for nitration, we repeated the experiment with a Y51F mutant of the heme domain (*39*). It was observed that RR signals associated with nitration of tyrosine residue(s) still developed, but much more slowly than with the wild-type heme domain, with RR signals increasing over several hours to reach their maximum. It appears that tyrosine 51 is a major target for nitration but that other tyrosine(s), presumably also in a hydrophobic location, are also modified over time. Effects of nitration on the catalytic properties of the wild-type and mutant P450s were also determined (see Effects of NO on P450 BM3 Catalysis section below).

Resonance Raman spectra for the Fe(III)NO complex of the P450 BM3 heme domain have been published previously. Our spectra are essentially identical to those published (*50*). However, RR spectra were also obtained for freeze−thawed solutions of the oxidized and aerobically NO-treated P450 domain (Figure 6). In the case of the nitric oxide-treated enzyme, the band patterns for nitrotyrosinate are particularly strong. However, for this species the core size marker bands of the heme for the low-spin form are at a remarkably high frequency, even for a low-spin heme [1597, 1514, and 1650 cm^{-1} (ν_2, ν_3, and ν_{10}, respectively); cf. 1581, 1499, and 1636 cm^{-1} for the oxidized, aqua-ligated P450]. This effect is typically observed when π-acid ligands (e.g., CO, NO) are bound to the axial positions of the hemes. In P450s the effect is not observed when the proximal cysteinate is bound, since the electron-donating properties of the thiolate ligand can compensate for the electron-withdrawing effect of the nitrosyl. Therefore, the marked shifts to higher frequency observed upon aerobic addition of NO and freeze−thawing the sample suggest that the proximal cysteinate is no longer bound to the heme. Band positions reported for the spectra of ferrous five-coordinate nitrosyl hemes are practically identical to the values observed here in the frozen solution (*54*). Therefore, the heme features of the spectrum in Figure 6B can be assigned to a ferrous five-coordinate nitrosyl complex of P450 BM3. It is conceivable that some autoreduction of the nitrosyl ferric heme occurs following aerobic exposure to an excess of nitric oxide. Autoreduction has been reported previously for certain hemoprotein complexes (*55*). The axial bond trans to the nitrosyl ligand in a ferrous heme complex is labile, and cleavage can occur easily. In the ferrous−nitrosyl complex, one electron occupies the dz^2 orbital. This is an antibonding orbital which weakens the other axial bond between the heme and the cysteine ligand. Cleavage could then be assisted by a conformational change in the protein induced by freezing. The binding of nitric oxide itself may induce a minor conformational change, as suggested by the zero-order nitric oxide release kinetics mentioned earlier. It has also been suggested that carbon monoxide might act as a conformational effector of P450 BM3 (*56*). However, the fact that the six-coordinate Fe(II)-NO P450 BM3 complex can be isolated in aqueous solution suggests that freezing is primarily responsible for breakage of the cysteinate linkage. As expected, when the frozen nitrosyl P450 complex was thawed and treated with reductant (dithionite) and carbon monoxide, the electronic absorption spectrum confirmed that it had been converted almost completely to the inactive P420 form.

Effects of NO on P450 BM3 Catalysis. In preliminary experiments, it was observed that addition of a few bubbles of nitric oxide to an assay solution of flavocytochrome P450 BM3 resulted in transient inactivation of fatty acid-dependent NADPH oxidation. Similar transient inactivation was observed on addition of small concentrations (ca. 1 mM) of the nitric oxide donor compound GSNO. However, the reductase domain-dependent rate of cytochrome *c* reduction was almost completely unaffected, indicating the specificity of nitric oxide for the P450 heme iron. When the nitric oxide-complexed flavocytochrome P450 BM3 (5 μM) was prepared and then diluted 100-fold into nitric oxide-free assay buffer for activity measurements (assay systems containing 50 nM enzyme in assay buffer at 30 °C with either 50 μM arachidonic acid or 800 μM lauric acid), virtually no inhibition was observed when the reaction was initiated by addition of 200 μM NADPH. This is likely to reflect considerable dissociation of nitric oxide from the heme iron into the aerobic buffer prior to the start of the assay. However, for arachidonic acid oxidation assays performed under identical conditions in the presence of a higher, measured concentration of nitric oxide [starting concentration of ca. 250 μM, produced by mixture of anaerobically generated NO-saturated (ca. 1.9 mM) buffer with oxygenated NO-free buffer containing P450 BM3 and arachidonate immediately prior to assay], almost complete inhibition of activity was observed on initiation of the reaction by NADPH addition. Thus, the initial rate (over the first 5 s) of arachidonic acid-dependent NADPH oxidation was ~14000 min^{-1} in the absence of nitric oxide, and <20 min^{-1} in its presence. Despite this initial inhibition, recovery of activity occurred rapidly during the course of the assay, such that the rate measured after ~45 s for the nitric oxide-treated enzyme was almost as high as that observed for the untreated P450. The relatively rapid recovery of activity indicates that the inhibitory NO could be displaced from the P450 heme under turnover conditions. This is consistent with our earlier results which indicated that NADPH-dependent electron transfer to the flavocytochrome P450 BM3 heme iron from its reductase domain was feasible in the Fe(III)NO species and that this reduction process displaced the nitrosyl ligand. The fact that P450-dependent fatty acid hydroxylation is oxygen-dependent means that it is difficult to extract meaningful kinetic parameters for the inhibition by NO (which reacts with oxygen in solution). However, it is clear that the transient inhibition of P450 BM3 results from coordination of the ferric heme iron by NO to form the Fe(III)NO complex and that inhibition is released as NO is displaced from the Fe(II)NO complex and reacts with oxygen in solution.

In view of the fact that resonance Raman studies indicated that aerobic incubation of P450 BM3 with nitric oxide induced nitration of tyrosine 51 (and probably one or more additional tyrosine residues), we determined the steady-state parameters for lauric acid-dependent oxidation of NADPH for wild-type and Y51F mutant flavocytochromes, both before and after aerobic incubation with nitric oxide. Prior to assays, enzymes (ca. 10 μM) were incubated for 1 h at 15 °C in 100 mM Tris·HCl (pH 7.5) both with and without the addition of nitric oxide (1 mM, by dilution of anaerobic stock solution). Over this time period, resonance Raman studies indicated essentially complete tyrosine nitration.

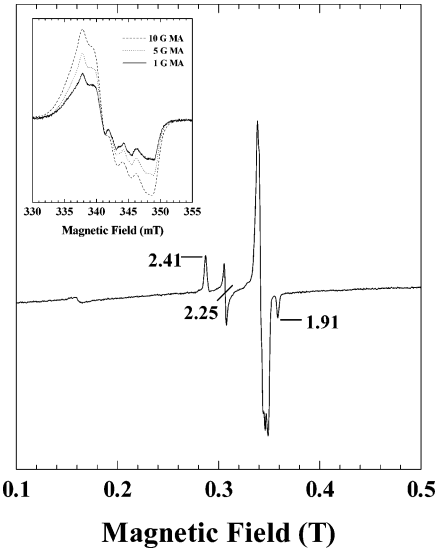

FIGURE 7: Perpendicular mode X-band EPR of ferrous cytochrome P450 BM3 plus nitric oxide in 50 mM HEPES/D_2O buffer (pH* 7.5). The protein concentration was 146 μM. EPR were recorded at 9.64 GHz with 2 mW power at 10 K. The modulation amplitude was 10 G. Inset: Effect of modulation amplitude on the hyperfine structure of the Fe(II)NO EPR spectrum. Microwave power and frequency are as above. The temperature was 23 K.

Enzyme solutions were then diluted 200-fold for assays. The kinetic properties of the untreated wild-type (k_{cat} = 5100 ± 75 min^{-1}; K_M = 280 ± 20 μM) and Y51F mutant (k_{cat} = 5900 ± 120 min^{-1}; K_M = 310 ± 20 μM) enzymes were similar to those we have reported previously (*39*). The activity of the nitric oxide-treated Y51F mutant enzyme was marginally affected with a 13% decrease in k_{cat} (k_{cat} = 5100 ± 140 min^{-1}; K_M = 270 ± 20 μM). However, the wild-type P450 was much more severely inhibited, with a 45% decrease in the k_{cat} value (k_{cat} = 2800 ± 80 min^{-1}; K_M = 200 ± 20 μM). Structural studies of P450 BM3 indicate that Y51 and R47 are key residues involved in the interaction with the carboxylate group of fatty acid substrates (*8*). Although a Y51F P450 BM3 mutant had rather small effects on kinetic parameters for laurate and arachidonate oxidation (*39*), nitration of Y51 would undoubtedly be expected to have a considerable effect on interaction with substrate carboxylate. Thus, our kinetic data for nitrated P450 BM3 enzymes are consistent with the proposed catalytic role of Y51.

EPR Studies. The X-band EPR spectrum of the wild-type P450 Fe(III)NO complex (not shown) contained only weak signals at g = 4.3, which can be assigned to adventitious iron, and a trace of ferrous nitrosyl signal centered at g = 2.0. The heme itself has been rendered EPR silent, as might be anticipated for the complete binding of a single NO molecule to each ferric ion. There are no signals arising from a low-spin Fe(III) species. When the EPR-silent ferrous wild-type P450 is exposed to NO under strict anaerobic conditions (as described in the Experimental Procedures section) and frozen for EPR spectroscopy, a rhombic spectrum with an apparent 3-fold splitting on the high-field g-value results (Figure 7). This Fe(II)NO ({FeNO}^{7}) signal is centered at g = 2.01. This feature is not identical to that reported previously for the Fe(II)NO form of P450 cam, which is rhombic with a three-line hyperfine centered at g = 2.002 (*57*, *58*). The nitrosyl feature retains the rhombic shape, but the hyperfine structure is less well resolved than in P450

cam. Large modulation amplitudes can cause line width broadening, but lower modulation amplitudes did not improve the resolution of the hyperfine in this case (Figure 7, inset). It is probable that this is due to heterogeneity in the conformation of the Fe(II)NO species. The perturbations observed in the electronic absorption spectra on addition of fatty acid substrate to the Fe(III)NO form suggest that bond deformation can occur.

Known Fe(II)NO heme EPR are essentially radical in origin, arising primarily from the bound NO ligand. The ferrous ion itself remains low-spin $S = 0$. Consequently, all *g*-values remain close to 2, as is also observed for the spectrum in Figure 7. When the NO is bound distal to histidine in proteins such as cytochrome cd_1 or horseradish peroxidase (HRP), the spectrum is rhombic with a nine-line hyperfine splitting on the central feature. This splitting arises because the unpaired spin interacts with the ($I = 1$) nitrogen nucleus of the NO and to a lesser extent with the nucleus of the coordinating nitrogen of histidine. In the absence of a distal histidine, the spectrum is axial with a 3-fold splitting on one feature [e.g., as seen for guanylate cyclase and cytochrome *c′* (*59*, *60*)]. Importantly, this Fe(II)NO P450 EPR spectrum is clearly not a three-line five-coordinate ferrous heme nitrosyl species, and this is taken as evidence that the cysteinate is still coordinated trans to NO in this form and that there is negligible P420 content (although freeze−thawing of the complex does generate P420). Signals at $g = 2.40$, 2.25, and 1.92 arise from a subpopulation of P450 that has reoxidized to the resting ferric form from the unstable wild-type P450 BM3 Fe(II)NO species (*35*), confirmed by measurements of the absorption spectrum following EPR.

The EPR spectrum for the Fe(II)NO adduct of the F393H heme domain mutant is essentially identical to that of wild-type P450 BM3, although in this case there are minimal signals arising from oxidized P450, as expected for the more stable Fe(II)NO adduct formed by this mutant (data not shown). Again, the signal is centered at $g = 2.01$ with 3-fold splitting.

MCD Spectroscopy. The spectrum shown for the Fe(III)-NO adduct of wild-type P450 BM3 (Figure 8A) is not consistent with heme in a low-spin ferric state but rather resembles that of low-spin ferrous heme. This is also common to the MCD spectra of the Fe(III)NO ($\{FeNO\}^6$) forms of myoglobin mutants and horseradish peroxidase, which also show band shapes and intensities normally associated with low-spin ferrous heme (*61*; see also ref *62* for a description of the metal−nitrosyl classification system]. The MCD spectra of the six- and five-coordinate Fe(III)NO derivatives of nitric oxide synthase (NOS), which also have thiolate ligation, have been published (*63*), and again these have a spectrum form that is associated with low-spin ferrous heme, although this was not commented upon by the authors. The position of the Soret crossover in cytochrome P450 BM3 is shifted to longer wavelength (crossover at 440 nm) relative to the myoglobin and peroxidase derivatives (ca. 420 nm) (*64*). This shift results from a change of the proximal heme ligand from histidine in the globins and peroxidases to a cysteine in P450. There is a derivative feature (Q-band) with a zero-line crossover at 574 nm and intensity of 54.5 M^{-1} cm^{-1} T^{-1}, which has a derivative-shaped vibrational side band at 541 nm. These are similar to the band positions and intensities observed for the Fe(III)NO derivation of NOS. To the best of our knowledge, this is the first MCD spectrum recorded for an Fe(III)NO derivative of a cytochrome P450.

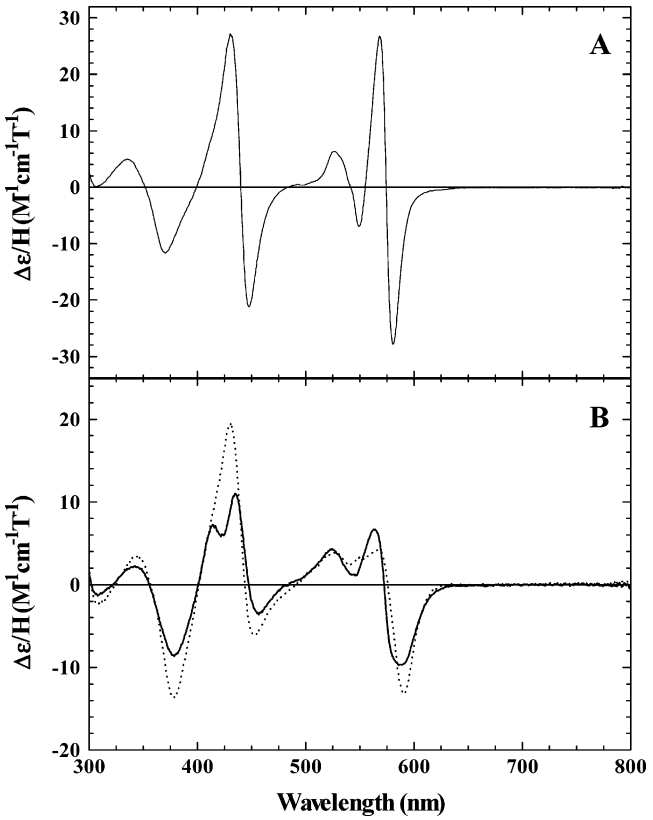

FIGURE 8: Room temperature MCD spectra for P450 BM3. Panel A shows the MCD spectrum for the Fe(III)NO complex of the wild-type P450 BM3 heme domain (110 μM). Panel B shows the spectra for the Fe(II)NO complexes of the wild-type (solid line, 148 μM) and F393H mutant (dotted line, 91 μM) BM3 heme domains. The F393H mutant shows complete conversion to the Fe(II)NO complex, whereas the wild-type heme domain spectrum is a spectral mixture of the Fe(II)NO species (ca. 48%) and reoxidized ferric P450. The spectra were collected at 298 K, 6 T, as described in the Experimental Procedures section.

The MCD spectrum of the Fe(II)NO form of wild-type cytochrome P450 BM3 is shown in Figure 8B. The Soret has a derivative crossover at 447 nm but shows two positive maxima at 414 and 434 nm. The intensity maximum at 414 nm can be assigned to the Fe(III) low-spin species observed in the absorbance and EPR spectra. The contribution of this oxidized species (52%) can be subtracted from the MCD, leaving a feature with a Soret crossover at 447 nm and a peak-to-trough intensity of 50.1 M^{-1} cm^{-1} T^{-1} at 100% population of Fe(II)NO heme. The Q-band derivative is centered at 574 nm and is calculated to have a peak-to-trough intensity of 34.4 M^{-1} cm^{-1} T^{-1}. The wavelengths of these bands are similar to those reported for Fe(II)NO derivatives of P450 cam (*58*, *61*, *64*) and NOS (*63*), and the calculated intensities of these bands in the P450 BM3 enzyme are slightly higher than those of the P450 cam spectra. The spectrum of the Fe(II)NO form of the mutant F393H is very similar in form and intensity to that of the wild-type difference spectrum: the Soret crossover is at 443.5 nm (peak-to-trough intensity 25 M^{-1} cm^{-1} T^{-1}), there is a peak at 527 nm, and the Q-band derivative is at 575 nm (17 M^{-1} cm^{-1} T^{-1}). Again, the positions of the bands are similar to those in the MCD spectrum of the wild-type P450 cam Fe-

(II)NO species, but the band intensity is lower in the spectrum of the P450 BM3 mutant. This does not suggest that the species is not fully converted to the ferrous nitrosyl species as the absorbance and EPR are consistent with full conversion. However, the broad Soret feature and lower intensity of the bands do suggest that there may be a variety of heme−nitrosyl conformations generating overlaying, but similar, spectra. Similar intensities were observed in the Fe(II)NO form of nitric oxide synthase. We can rule out the formation of five-coordinate heme nitrosyl heme at room temperature as these species have negative Soret features at around 400 nm (*61*, *65*).

Comparison of the MCD spectra reported for the NO derivative of ferrous P450 cam and the spectra presented here for P450 BM3 shows that their nitric oxide heme derivatives have MCD spectra that distinguish Fe(III)NO and Fe(II)NO forms of the cysteine-ligated heme. Both the Soret and Q-bands of Fe(II)NO cysteine-ligated hemes become asymmetric, which is a pattern similar to the spectra of nitrosyl hemes with proximal histidine ligation (*63*).

DISCUSSION

Our study presents the first MCD spectra for a six-coordinate Fe(III)NO cytochrome P450 complex and the first CD spectrum for a P450 in the Fe(II)NO form. In addition, we demonstrate that resonance Raman spectroscopy provides a straightforward and sensitive method for identifying nitrated tyrosine residues in enzymes. Given the interest in nitration of tyrosine residues in relation to, for example, signal transduction, cellular inflammation, neurodegeneration, and enzyme inhibition (e.g., refs *66*−*71*), the technique may now find more widespread use in the analysis of nitrated proteins. While a biological role for tyrosine nitration in P450 BM3 is not known, the fact that interaction with nitric oxide leads to both transient enzyme inactivation (through ligation to ferric heme iron) and long-term inhibition (likely through tyrosine nitration), which is similar to the behavior reported for other mammalian P450 enzymes (e.g., refs *69* and *70*), indicates that this general phenomenon is of physiological relevance with regard to control of P450 activity.

Through a combination of spectroscopic and enzymology studies, we have demonstrated that transient inhibition of flavocytochrome P450 BM3 activity is associated with ligation of nitric oxide to the ferric heme iron and that this species can be reduced by electron transfer from the physiological cofactor NADPH through the reductase domain of the enzyme. The resulting Fe(II)NO adduct is unstable and breaks down, releasing nitric oxide and allowing restoration of catalytic activity. Our experiments demonstrate release of NO both through NADPH-dependent reduction of flavocytochrome P450 BM3 and by flavodoxin semiquinone-dependent reduction of the heme (proven by subsequent trapping of the NO released) and provide evidence that aerobic single-electron reduction of NO-bound P450 BM3 induces the loss of NO itself, as opposed to, e.g., NO^- or N_2O. Fungal P450 nor produces N_2O by the direct reduction of the NO-bound P450 by NADH, consuming 2 equiv of NO in the reaction (*4*). A similar situation is unlikely in the BM3 enzyme, since reduction of a stoichiometric P450−NO complex still results in NO displacement and since NAD(P)H cannot reduce directly the Fe(III)NO P450 BM3 heme domain.

Resonance Raman studies indicate that, over a period of several minutes, aerobic interaction with nitric oxide results in the nitration of tyrosine residue(s) in P450 BM3. The fact that this occurs over the same time frame as the spontaneous reoxidation of the ferric−nitrosyl adduct of the enzyme suggests that nitric oxide released within the hydrophobic active site cavity of the enzyme may be the main originator of tyrosine nitration. Steady-state kinetic studies reveal inhibition of fatty acid hydroxylase activity after aerobic treatment with nitric oxide, and it appears to be the case that nitration of internal tyrosine residue(s) is the explanation for this long-term inhibitory effect, as observed for other mammalian P450s (e.g., refs *70* and *71*). No nitrotyrosine signal was observed after anaerobic reaction, indicating the requirement for oxygen in this process. On aerobic reoxidation of the Fe(III)NO adduct of wild-type flavocytochrome P450 BM3, fatty acid hydroxylase activity (k_{cat} for lauric acid hydroxylation) falls to almost half of its original value. However, cytochrome *c* reduction associated with its reductase domain is virtually unaffected, indicating that the effect is specific for the heme domain of the enzyme. The much slower nitration observed for BM3 mutant Y51F, coupled with the fact that its activity is decreased by only 13%, indicates that tyrosine 51 is a likely major (but not exclusive) target for nitration. This partial irreversible inhibitory effect of nitric oxide on P450 BM3 is similar to the phenomenon observed with mammalian P450s 2B4 and 1A1 and for the other hemoproteins cyclooxygenase and lipooxygenase (*70*, *71*). Our data suggest that tyrosine nitration in P450 BM3 is the mechanism by which NO mediates an irreversible inactivation of the enzyme. We can speculate that similar tyrosine nitration event(s) underlie(s) the irreversible inactivation of the other hemoproteins mentioned, and this suggestion is supported by our demonstration of tyrosine nitration in P450 2B4 (*30*). The nature of the SERR signal for nitrotyrosine of P450 BM3 indicates that the residue(s) modified is (are) not surface exposed, since the frequency of the symmetric stretching vibration of the nitro group is at a much lower wavenumber than that for aqueous nitrotyrosinate. In superoxide dismutase, the peroxynitrite-mediated nitration of a surface tyrosine resulted in a resonance Raman band at 1336 cm^{-1}, the same as that observed for free nitrotyrosinate (*72*). In hen egg white lysozyme, treatment with tetranitromethane resulted in distinct resonance Raman signals for nitrotyrosinate at 1336 and 1328 cm^{-1}. The former vibration is associated with a surface tyrosinate, while the latter is from a tyrosinate in a strongly hydrophobic environment, as indicated by the fact that signals for free nitrotyrosinate in aqueous and organic solvents are located at 1336 and 1328 cm^{-1}, respectively (*73*). The nitrotyrosinate signal from P450 BM3 is sharp and located at 1328 cm^{-1}, suggesting that it might reflect only a single modified tyrosine in a hydrophobic environment. Our studies indicate that tyrosine 51 is a nitration target but that there may be one or more further tyrosine targets. Since the reaction of NO with P450 BM3 tyrosine(s) is oxygen-dependent, the active oxidant is clearly a higher oxide of nitrogen. Possible candidates are peroxynitrite, nitrogen dioxide, and dinitrogen trioxide. While peroxynitrite has attracted much attention as a damaging oxidant, it is a hydrophilic species and perhaps unlikely to bring about nitration of an internal tyrosine. By contrast, NO_2 and N_2O_3 are more lipophilic agents and

perhaps more likely nitrating agents. Recently, Ullrich and co-workers have described the nitration of tyrosine 334 following additions of peroxynitrite to flavocytochrome P450 BM3 (*29*). While we cannot rule out the possibility that Y334 is nitrated in addition to Y51 following aerobic incubation with nitric oxide, this seems unlikely due to the location of Y334 at the entrance of an aqueous channel to the heme. Thus, the nitro group vibrational signal from nitrotyrosine 334 would be expected at higher wavenumber than was observed in our study. Clearly, modification of P450 BM3 by peroxynitrite and by nitric oxide results in distinct nitration events.

The electronic absorption properties we present here for the nitrosyl complexes of ferric and ferrous forms of P450 BM3 are similar, but not identical, to those reported previously for P450 cam (Table 1). In particular, the Soret band for the Fe(III)NO complex is shifted by 5 nm to longer wavelength than the corresponding band in P450 cam. In both P450s, the Fe(II)NO species is unstable and is isolated only under anaerobic conditions. The instability of Fe(II)-NO P450 complexes has also been reported for microsomal forms of P450. However, these results contrast with the behavior of the nitric oxide synthase (NOS) enzymes, which are also cysteinate-ligated heme *b* (protoporphyrin IX)-containing cytochromes (*44*). In NOS, the ligation of the nitric oxide product to the ferrous heme iron is thought to be responsible for limiting catalytic activity. In steady-state turnover, a considerable proportion of NOS (70−90% for the neuronal form) is in the inhibited Fe(II)NO complex (*74*). This points to different electronic properties of the heme systems in the two enzyme classes, despite similar iron ligation. In recent work, it was shown that mutation of the phenylalanine residue phylogenetically conserved in the P450 superfamily heme-binding motif (F393 in P450 BM3) has profound effects on the electronegativity of the BM3 heme iron (*40*). The heme iron reduction potential in mutant enzyme F393H was elevated by 95 mV relative to the wild-type BM3 (to −332 mV versus SHE), suggesting that the electron density on the heme iron is decreased and explaining the higher stability of the ferrous form of this mutant. The more positive heme reduction potential in BM3 F393H is now much more similar to those of NOS isoforms [e.g., −248 mV for nNOS, −295 mV for iNOS (*44*)], and we show here that the F393H mutant also behaves in a more NOS-like fashion by stabilizing the Fe(II)NO complex to a much greater degree than does the wild-type P450 BM3. The enhanced stability of the Fe(II)NO form in the F393H mutant has enabled us to characterize this P450 species spectroscopically with relative ease (Figures 1−4 and 8).

As has been observed previously for mammalian P450 (*17*), the iron−cysteinate bond of the P450 BM3 nitrosyl complex is relatively labile, and freeze−thawing of the Fe(III)−NO heme domain complex formed by aerobic treatment with excess nitric oxide leads to scission of this bond, as determined here by resonance Raman. It should be noted here that nitric oxide-induced release of axial histidine ligation to heme iron is exploited naturally for the activation of the key signaling enzyme guanylate cyclase (*60*, *75*). However, perhaps the most interesting feature observed from the study of the electronic absorption properties of the P450 BM3 nitrosyl adducts is the fact that addition of fatty acid substrate perturbs the Fe(III)NO spectrum. Should this phenomenon prove to be common among the P450s, then it may be a useful means of probing their active sites and/or screening for P450−drug interactions. Thus, if molecules binding to a P450 active site (but not ligating to the heme iron) do not elicit a spectral change per se, it is conceivable that they may do so indirectly by effects on the nature of the iron−nitrosyl bond. In ongoing spectroscopic studies, we are examining further the interaction of P450 BM3−nitrosyl adducts with lipids and other molecules in order to probe molecular interactions in the active site of wild-type and mutant forms.

Finally, as a result of the detailed spectroscopic and kinetic analyses of the Fe(III)NO and Fe(II)NO species of wild-type and mutant P450s BM3 presented in this study, we are able to make important comparisons between the relative stabilities of these species and with their counterparts in the related nitric oxide synthases. In P450 BM3 (as in NOS), the Fe(III)NO species is quite stable. In aerobic solution it decays very slowly due primarily to the irreversible reaction of free NO with O_2 in solution. However, the Fe(II)NO species of wild-type P450 BM3 is unstable and collapses rapidly to a mixture of Fe(III) and Fe(III)NO species under aerobic conditions and under anaerobic conditions to an apparently more complex mixture of ferric and ferrous forms, a minor proportion of which are NO-coordinated. The presence of oxygen is evidently not the cause of the instability of the Fe(II)NO complex. By contrast, the Fe(II)NO complex of the F393H mutant is more stable. The difference in stabilities of the wild-type and F393H mutant complexes is not simply rationalized on the basis of the apparent NO binding (k_{on}) and dissociation (k_{off}) rates determined from stopped-flow binding studies, since the k_{on} is rather faster than the k_{off} under the conditions examined (e.g., for wild-type P450 BM3 apparent k_{on} values are between 46 and 467 s^{-1} between 10 and 100 μM NO, while apparent k_{off} is $\sim$14 s^{-1}). Thus, it might be expected that the Fe(II)NO form would predominate for both wild-type and F393H P450 BM3. However, a factor which must be considered is that the ferrous form of the wild-type P450 BM3 is an effective scavenger of oxygen and reacts rapidly to regenerate the stable ferric heme iron state (*35*, *45*). In contrast, the reduction of the wild-type P450 BM3 heme domain is rather slow for both kinetic and thermodynamic reasons. The midpoint potential of dithionite is rather similar to that for the substrate-free P450 BM3 heme iron (*45*). In anaerobic studies of dithionite-dependent reduction of the wild-type P450 BM3, full reduction of the heme iron takes several minutes even when dithionite is in large excess. Thus, it appears that competing reactions [i.e., NO binding, NO dissociation, ferrous heme iron reoxidation, and (where dithionite is present) dithionite-dependent reduction of ferric and Fe(III)NO P450] lead to the formation of a mixture of species for wild-type P450 BM3. In the case of the F393H mutant, its much more positive heme iron reduction potential and more stable ferrous form likely result in the higher stability of the Fe(II)NO complex. While freeze−thawing of P450 BM3 leads to loss of cysteinate ligation, formation of the Fe(II)NO species per se does not result in P420 formation, as evidenced both from MCD/EPR studies and from the fact that CO-binding studies result in near-stoichiometric formation of a P450 complex. These findings indicate important differences in the behavior of P450 BM3

by comparison with NOS isoforms. In iNOS, for instance, the binding of NO to the ferrous heme iron results in transient formation of an Fe(II)NO species, which collapses rapidly (*46*). However, the nature of this species is different from that seen for P450 BM3. In iNOS the absorption of this species at 396 nm identifies it as a five-coordinate ferrous−nitrosyl complex (e.g., refs *46* and *76*). In P450 BM3, there is no spectroscopic evidence for such a complex, and it is likely that cysteinate ligation remains intact following Fe(II)NO formation. Our work here and previous studies by Shimizu and co-workers (*77*) have identified residues important to stability of P450 nitrosyl complexes, and it is likely that the NOS isoforms have evolved differently from the P450s to incorporate residues about the heme that finely tune its reactivity with NO and possibly its ability to self-regulate NO production through transient and reversible formation of both five-coordinate and six-coordinate Fe(II)-NO complexes (*78*). Thus, despite similarities in heme coordination and reaction chemistry, important differences between P450 BM3 and its flavocytochrome NOS relatives are evident from these studies of P450 BM3 reactivity with nitric oxide.

ACKNOWLEDGMENT

We are grateful to the late Professor Therese Cotton (Iowa State University) for provision of access to Raman facilities in her laboratory.

REFERENCES

1. Munro, A. W., and Lindsay, J. G. (1996) Bacterial cytochromes P450, *Mol. Microbiol. 20*, 1115−1125.
2. Lee-Robichaud, P., Akhtar, M. E., and Akhtar, M. (1998) Control of androgen biosynthesis in the human through the interaction of Arg^{347} and Arg^{358} of CYP17 with cytochrome b_5, *Biochem. J. 332*, 293−296.
3. Guengerich, F. P. (1995) Human cytochrome P450 enzymes, in *Cytochrome P450: Structure, function and mechanism* (Ortiz de Montellano, P. R., Ed.) pp 473−535, Plenum Press, New York.
4. Park, S. Y., Shimizu, H., Adachi, S., Nakagawa, A., Tanaka, A., Nakahara, K., Shoun, H., Obayashi, E., Nakamura, H., Izuka, T., and Shiro, Y. (1997) Crystal structure of nitric oxide reductase from denitrifying fungus *Fusarium oxysporum*, *Nat. Struct. Biol. 4*, 827−832.
5. Ravichandran, K. G., Boddupalli, S. S., Hasemann, C. A., Peterson, J. A., and Deisenhofer, J. (1993) Crystal structure of hemoprotein domain of P450 BM-3, a prototype for microsomal P450s, *Science 261*, 731−736.
6. Watanabe, I., Nara, F., and Serizawa, N. (1995) Cloning, characterization and expression of the gene encoding cytochrome P450 sca2 from *Streptomyces carbophilus* involved in production of pravastatin, a specific HMG-CoA reductase inhibitor, *Gene 163*, 81−85.
7. Poulos, T. L., Finzel, B. C., and Howard, A. J. (1987) High-resolution structure of cytochrome P450 cam, *J. Mol. Biol. 195*, 687−700.
8. Li, H.-Y., and Poulos, T. L. (1997) The structure of cytochrome P450 BM3 haem domain complexed with the fatty acid substrate, palmitoleic acid, *Nat. Struct. Biol. 4*, 140−146.
9. Raag, R., Li, H., Jones, B. C., and Poulos, T. L. (1993) Inhibitor-induced conformational change in cytochrome P450 cam, *Biochemistry 32*, 4571−4578.
10. Cupp-Vickery, J. R., Han, O., Hutchinson, C. R., and Poulos, T. L. (1996) Substrate-assisted catalysis in cytochrome P450eryF, *Nat. Struct. Biol. 3*, 632−637.
11. Williams, P. A., Cosme, J., Sridhar, V., Johnson, E. F., and McRee, D. E. (2000) Mammalian microsomal cytochrome P450 monooxygenase: Structural adaptations for membrane binding and functional diversity, *Mol. Cell 5*, 121−131.
12. Cosme, J., and Johnson, E. F. (2000) Engineering microsomal cytochrome P450 2C5 to be a soluble, monomeric enzyme−mutations that alter aggregation, phospholipid dependence of catalysis, and membrane binding, *J. Biol. Chem. 275*, 2545−2533.
13. Wester, M. R., Johnson, E. F., Marques-Soares, C., Dansette, P. M., Mansuy, D., and Stout, C. D. (2003) Structure of a substrate complex of mammalian cytochrome P450 2C5 at 2.3 Å resolution: Evidence for multiple substrate-binding modes, *Biochemistry 42*, 6370−6379.
14. Williams, P. A., Cosme, J., Ward, A., Angove, H. C., Matak Vinkovic, D., and Jhoti, H. (2003) Crystal structure of human cytochrome P450 2C9 with bound warfarin, *Nature 424*, 464−468.
15. Narhi, L. O., and Fulco, A. J. (1987) Identification and characterization of two functional domains in cytochrome P-450 BM-3, a catalytically self-sufficient monooxygenase induced by barbiturates in *Bacillus megaterium*, *J. Biol. Chem. 262*, 6683−6690.
16. Nobel Foundation at http://www.nobel.se/medicine/laureates/1998/index.html.
17. Ignarro, L. J. (1999) Nitric oxide: A unique endogenous signaling molecule in vascular biology, *Angew. Chem., Int. Ed. 38*, 1882−1892.
18. Donovan, M., Carmody, R. J., and Cotter, T. G. (2001) Light-induced photoreceptor apoptosis *in vivo* requires neuronal nitric oxide synthase and guanylate cyclase activity, and is caspase-3 independent, *J. Biol. Chem. 276*, 23000−23008.
19. O'Keefe, D. H., Ebel, R. E., and Peterson, J. A. (1978) Studies of the oxygen binding site of cytochrome P-450: nitric oxide as a spin-label probe, *J. Biol. Chem. 253*, 3509−3516.
20. Obayashi, E., Tsukamoto, K., Adachi, S., Takahashi, S., Nomura, M., Izuka, T., Shoun, H., and Shiro, Y. (1997) Unique binding of nitric oxide to ferric nitric oxide reductase from *Fusarium oxysporum* elucidated with infrared, resonance Raman, and X-ray absorption spectroscopies, *J. Am. Chem. Soc. 119*, 7807−7816.
21. Ignarro, L. J., Adams, J. B., Horwitz, P. M., and Wood, K. S. (1986) Activation of soluble guanylate cyclase by NO-hemoproteins involves NO-heme exchange. Comparison of heme-containing and heme-deficient enzyme forms, *J. Biol. Chem. 261*, 4997−5002.
22. Stuehr, D. J., Cho, H. J., Kwon, N. S., Weise, M. F., and Nathan, C. F. (1991) Purification and characterization of the cytokine-induced macrophage nitric oxide synthase−an FAD-containing and FMN-containing flavoprotein, *Proc. Natl. Acad. Sci. U.S.A. 88*, 7773−7777.
23. Wang, J., Rousseau, D. L., Abu-Soud, H. M., and Stuehr, D. J. (1994) Heme coordination of NO in NO synthase, *Proc. Natl. Acad. Sci. U.S.A. 91*, 10512−10516.
24. Gorren, A. C. F., Schrammel, A., Riethmuller, C., Schmidt, K., Koesling, D., Werner, E. R., and Mayer, B. (2000) Nitric oxide-induced autoinhibition of neuronal nitric oxide synthase in the presence of the autoxidation-resistant pteridine 5-methyltetrahydrobiopterin, *Biochem. J. 347*, 475−483.
25. Hanke, C. J., Drewett, J. G., Myers, C. R., and Campbell, W. B. (1998) Nitric oxide inhibits aldosterone synthesis by a guanylyl cyclase-independent effect, *Endocrinology 139*, 4053−4060.
26. Adams, M. L., Meyer, E. R., Sewing, B. N., and Cicero, T. J. (1994) Effects of nitric oxide-related agents on rat testicular function, *J. Pharmacol. Exp. Ther. 269*, 230−237.
27. Kanner, J., Harel, S., and Granit, R. (1992) Nitric oxide, an inhibitor of lipid oxidation by lipoxygenase, cyclooxygenase and hemoglobin, *Lipids 27*, 46−49.
28. Wink, D. A., Osawa, Y., Darbyshire, J. F., Jones, C. R., Eshenaur, S. C., and Nims, R. W. (1993) Inhibition of cytochromes P450 by nitric oxide and a nitric oxide-releasing agent, *Arch. Biochem. Biophys. 300*, 115−123.
29. Snyder, G. D., Holmes, R. W., Bates, J. N., and van Voorhis, B. J. (1996) Nitric oxide inhibits aromatase activity: Mechanisms of action, *J. Steroid Biochem. Mol. Biol. 58*, 63−69.
30. Quaroni, L., Reglinski, J., Wolf, R., and Smith, W. E. (1996) Interaction of nitrogen monoxide with cytochrome P450 monitored by surface-enhanced resonance Raman scattering, *Biochim. Biophys. Acta 1296*, 5−8.
31. Daiber, A., Herold, S., Schoneich, C., Namgaladze, D., Peterson, J. A., and Ullrich, V. (2000) Nitration and inactivation of P450 BM3 by peroxynitrite−stopped flow measurements prove ferryl intermediates, *Eur. J. Biochem. 267*, 6729−6739.
32. Zou, M. H., Yesilkaya, A., and Ullrich, V. (1999) Peroxynitrite inactivates prostacyclin synthase by heme-thiolate-catalyzed tyrosine nitration, *Drug Metab. Rev. 31*, 343−349.

33. Ricoux, R., Boucher, J.-L., Mansuy, D., and Mahy, J.-P. (2001) Microperoxidase 8 catalyzed nitration of phenol by nitrogen dioxide radicals, *Eur. J. Biochem. 268*, 3783−3788.
34. Pfeiffer, S., Lass, A., Schmidt, K., and Mayer, B. (2001) Protein tyrosine nitration in cytokine-activated murine macrophages. Involvement of a peroxidase/nitrite pathway rather than peroxynitrite, *J. Biol. Chem. 276*, 34051−34058.
35. Miles, J. S., Munro, A. W., Rospendowski, B. N., Smith, W. E., McKnight, J., and Thomson, A. J. (1992) Domains of the catalytically self-sufficient cytochrome P450 BM3−genetic construction, overexpression, purification and spectroscopic characterization, *Biochem. J. 288*, 503−509.
36. Munro, A. W., Lindsay, J. G., Coggins, J. R., Kelly, S. M., and Price, N. C. (1994) Structural and enzymological analysis of the interaction of isolated domains of cytochrome P450 BM3, *FEBS Lett. 343*, 70−74.
37. Kunkel, T. A. (1985) Rapid and efficient site-specific mutagenesis without phenotypic selection, *Proc. Natl. Acad. Sci. U.S.A. 82*, 488−492.
38. Zoller, M. J., and Smith, M. (1983) Oligonucleotide-directed mutagenesis of DNA fragments cloned into M13 vectors, *Methods Enzymol. 100*, 468−500.
39. Noble, M. A., Miles, C. S., Chapman, S. K., Lysek, D. A., Mackay, A. C., Reid, G. A., Hanzlik, R. P., and Munro, A. W. (1999) Roles of key active site residues in flavocytochrome P450 BM3, *Biochem. J. 339*, 371−379.
40. Ost, T. W. B., Miles, C. S., Munro, A. W., Murdoch, J., Reid, G. A., and Chapman, S. K. (2001) Phenylalanine 393 exerts thermodynamic control over the heme of flavocytochrome P450 BM3, *Biochemistry 40*, 13421−13429.
41. Kosan, V. B., Fridman, M. T., and Kafarov, V. V. (1963) in *The solubilities of inorganic and organic compounds* (Stephen, H., and Stephen, T., Eds.) p 30, Pergamon Press, Oxford, U.K.
42. McIver, L., Leadbeater, C., Campopiano, D. J., Baxter, R. L., Daff, S. N., Chapman, S. K., and Munro, A. W. (1998) Characterisation of flavodoxin $NADP^+$ oxidoreductase and flavodoxin: key components of electron transfer in *Escherichia coli*, *Eur. J. Biochem. 257*, 577−585.
43. Lee, P. C., and Meisel, D. (1982) Adsorption and surface-enhanced Raman of dyes on silver and gold sols, *J. Phys. Chem. 86*, 3391−3395.
44. Daff, S., Noble, M. A., Craig, D. H., Rivers, S. L., Chapman, S. K., Munro, A. W., Fujiwara, S., Rozhkova, E., Sagami, I., and Shimizu, T. (2001) Control of electron transfer in neuronal NO synthase, *Biochem. Soc. Trans. 29*, 147−152.
45. Daff, S. N., Chapman, S. K., Turner, K. L., Holt, R. A., Govindaraj, S., Poulos, T. L., and Munro, A. W. (1997) Redox control of the catalytic cycle of flavocytochrome P450 BM3, *Biochemistry 36*, 13816−13823.
46. Abu-Soud, H. M., Wu, C., Ghosh, D. K., and Stuehr, D. J. (1998) Stopped-flow analysis of CO and NO binding to inducible nitric oxide synthase, *Biochemistry 37*, 3777−3786.
47. Graham-Lorence, S., Truan, G., Peterson, J. A., Falck, J. R., Wei, S., Helvig, C., and Capdevila, J. H. (1997) An active site substitution, F87V, converts cytochrome P450 BM-3 into a regio- and stereoselective (14S, 15R)-arachidonic acid epoxygenase, *J. Biol. Chem. 272*, 1127−1135.
48. Girvan, H. M., Marshall, K. R., Lawson, R. J., Leys, D., Joyce, M. G., Clarkson, J., Smith, W. E., Cheesman, M. R., and Munro, A. W. (2004) Flavocytochrome P450 BM3 mutant A264E undergoes substrate-dependent formation of a novel heme iron ligand set, *J. Biol. Chem. 279*, 23274−23286.
49. Joyce, M. G., Girvan, H. M., Munro, A. W., and Leys, D. (2004) A single mutation in P450 BM3 induces the conformational rearrangement seen upon substrate-binding in wild-type enzyme, *J. Biol. Chem. 279*, 23287−23293.
50. Deng, T. J., Proniewicz, L. M., Kincaid, J. R., Yeom, H., Macdonald, I. D. G., and Sligar, S. G. (1999) Resonance Raman studies of cytochrome P450 BM3 and its complexes with exogenous ligands, *Biochemistry 38*, 13699−13706.
51. Macdonald, I. D. G., Munro, A. W., and Smith, W. E. (1998) Fatty acid-induced alteration of the porphyrin macrocycle of cytochrome P450 BM3, *Biophys. J. 74*, 3241−3249.
52. Macdonald, I. D. G., Smith, W. E., and Munro, A. W. (1998) Inhibitor/fatty acid interactions with cytochrome P450 BM3, *FEBS Lett. 396*, 196−200.
53. Quaroni, L. G., and Smith, W. E. (1999) The nitro stretch as a probe of the environment of nitrophenols and nitrotyrosines, *J. Raman Spectrosc. 30*, 537−542.
54. Nagai, K., Welborn, C., Dolphin, D., and Kitagawa, T. (1980) Resonance Raman evidence for cleavage of the $Fe-N_\epsilon$ (His-F8) bond in the alpha subunit of the T-structure nitrosylhemoglobin, *Biochemistry 19*, 4755−4761.
55. Addison, A. W., and Stephanos, J. J. (1986) Nitrosyl Fe(III) hemoglobin: autoreduction and spectroscopy, *Biochemistry 25*, 4104−4113.
56. Murataliev, M. B., and Feyereisen, R. (1996) Functional interactions in cytochrome P450 BM3. Fatty acid substrate binding alters electron-transfer properties of the flavoprotein domain, *Biochemistry 35*, 15029−15037.
57. Dawson, J. H., Andersson, L. A., and Sono, M. (1983) Circular dichroism studies of low-spin ferric cytochrome P450 cam ligand complexes, *J. Biol. Chem. 258*, 13637−13645.
58. Ebel, R. E., O'Keefe, D. H., and Peterson, J. A. (1975) Nitric oxide complexes of cytochrome P-450, *FEBS Lett. 55*, 198−201.
59. Suzuki, S., Yoshimura, T., Nakahara, A., Iwasaki, H., Shidara, S., and Matsubara, T. (1987) Electronic and magnetic circular dichroism spectra of pentacoordinate nitrosyl hemes in cytochrome *c*′ from nonphotosynthetic bacteria and their model complexes, *Inorg. Chem. 26*, 1006−1008.
60. Stone, J. R., Sands, R. H., Dunham, W. R., and Marletta, M. A. (1995) Electron paramagnetic resonance spectral evidence for the formation of a pentacoordinate nitrosyl heme complex on soluble guanylate cyclase, *Biochem. Biophys. Res. Commun. 207*, 572−577.
61. Seward, H. E. (1999) Magneto-optical spectroscopy of hemoproteins, Ph.D. Thesis, University of East Anglia, U.K.
62. Enemark, J. H., and Feltham, R. D. (1974) Principles of structure, bonding and reactivity for metal nitrosyl complexes, *Coord. Chem. Rev. 13*, 339−346.
63. Voegtle, H. L., Sono, M., Adak, S., Pond, A. E., Tomita, T., Perera, R., Goodin, D. B., Ikeda-Saito, M., Stuehr, D. J., and Dawson, J. H. (2003) Spectroscopic characterization of five- and six-coordinate ferrous-NO heme complexes: Evidence for heme Fe-proximal cysteinate bond cleavage in the ferrous-NO adducts of Trp/Phe proximal environmental mutants of neuronal nitric oxide synthase, *Biochemistry 42*, 2475−2484.
64. Sono, M., Eble, K. S., Dawson, J. H., and Hager, L. P. (1985) Preparation and properties of ferrous chloroperoxidase complexes with dioxygen, nitric oxide and an alkyl isocyanide—spectroscopic dissimilarities between the oxygenated forms of chloroperoxidase and cytochrome P450, *J. Biol. Chem. 260*, 5530−5535.
65. Shimuzu, T., Iizuka, T., Shimada, H., Ishimura, Y., Nozawa, T., and Hatano, M. (1981) Magnetic circular dichroism studies of cytochrome P450 cam: Characterization of axial ligands of ferric and ferrous low-spin complexes, *Biochim. Biophys. Acta 670*, 341−354.
66. Berlett, B. S., Friguet, B., Yim, M. B., Chock, P. B., and Stadtman, E. R. (1996) Peroxynitrite-mediated nitration of tyrosine residues in *Escherichia coli* glutamine synthetase mimics adenylation: Relevance to signal transduction, *Proc. Natl. Acad. Sci. U.S.A. 93*, 1776−1780.
67. Marcondes, S., Turko, I. V., and Murad, F. (2001) Nitration of succinyl-CoA: 3-oxoacid CoA-transferase in rats after endotoxin administration, *Proc. Natl. Acad. Sci. U.S.A. 98*, 7146−7151.
68. Mihm, M. J., Schanbacher, B. L., Wallace, B. L., Wallace, L. J., Uretsky, N. J., and Bauer, J. A. (2001) Free 3-nitrotyrosine causes striatal neurodegeneration *in vivo*, *J. Neurosci. 21*, U11−U15.
69. Roberts, E. S., Lin, H. L., Crowley, J. R., Vuletich, J. L., Osawa, Y., and Hollenberg, P. F. (1998) Peroxynitrite mediated nitration of tyrosine and inactivation of the catalytic activity of cytochrome P450 2B1, *Chem. Res. Toxicol. 11*, 1067−1074.
70. Wink, D. A., Osawa, Y., Darbyshire, J. F., Jones, C. R., Eshenauer, S. C., and Nims, R. W. (1993) Inhibition of cytochromes P450 by nitric oxide and a nitric oxide releasing agent, *Arch. Biochem. Biophys. 300*, 115−123.
71. Kanner, J., Harel, S., and Granit, R. (1992) Nitric oxide, an inhibitor of lipid oxidation by lipoxygenase, cyclooxygenase and hemoglobin, *Lipids 27*, 46−49.
72. Ischiropoulos, H., Zhu, L., Chen, J., Tsai, M., Martin, J. C., Smith, C. D., and Beckman, J. S. (1992) Peroxynitrite-mediated tyrosine nitration catalyzed by superoxide dismutase, *Arch. Biochem. Biophys. 298*, 431−437.
73. Yamada, H., Yamashita, T., Domoto, H., and Imoto, T. (1990) Reaction of hen egg white lysozyme with tetranitromethane—a new side reaction, oxygen bond cleavage at glycine 104, and sequential nitration of 3 tyrosine residues, *J. Biochem. 108*, 432−440.

74. Abu Soud, H. M., Wang, J. L., Rousseau, D. L., Fukuto, J. M., Ignarro, L. J., and Stuehr, D. J. (1995) Neuronal nitric oxide synthase self-inactivates by forming a ferrous-nitrosyl complex during aerobic catalysis, *J. Biol. Chem. 270*, 22997−23006.
75. Zhao, Y., Brandish, P. E., Ballou, D. P., and Marletta, M. A. (1999) A molecular basis for nitric oxide sensing by soluble guanylate cyclase, *Proc. Natl. Acad. Sci. U.S.A. 96*, 14753−14758.
76. Stone, J. R., and Marletta, M. A. (1994) Soluble guanylate cyclase from bovine lung: activation with nitric oxide and carbon monoxide and spectral characterization of the ferrous and ferric states, *Biochemistry 33*, 5636−5640.
77. Nakano, R., Sato, H., Watanabe, A., Ito, O., and Shimizu, T. (1996) Conserved Glu^{318} at the cytochrome P450 1A2 distal site is crucial to the nitric oxide complex stability, *J. Biol. Chem. 271*, 8570−8574.
78. Stuehr, D. J., Santolini, J., Wang, Z.-Q., Wei, C.-C., and Adak, S. (2004) Update on mechanism and catalytic regulation in the NO synthases, *J. Biol. Chem. 279*, 36167−36170.
79. White, R. E., and Coon, M. J. (1982) Heme ligand replacement reactions of cytochrome P-450, *J. Biol. Chem. 257*, 3073−3078.
80. Hurshman, A. R., and Marletta, M. A. (1995) Nitric oxide complexes of inducible nitric oxide synthase: spectral characterization and effect on catalytic activity, *Biochemistry 34*, 5627−5634.

BI049163G